J Physiol 0.0 (2024) pp 1–22

The Journal of Physiology

Conserved mammalian muscle mechanics during eccentric contractions

Roger W. P. Kissane[1] and Graham N. Askew[2]

[1]*Department of Musculoskeletal & Ageing Science, University of Liverpool, Liverpool, UK*
[2]*School of Biomedical Sciences, University of Leeds, Leeds, UK*

Handling Editors: Paul Greenhaff & Martino Franchi

The peer review history is available in the Supporting Information section of this article (https://doi.org/10.1113/JP285549#support-information-section).

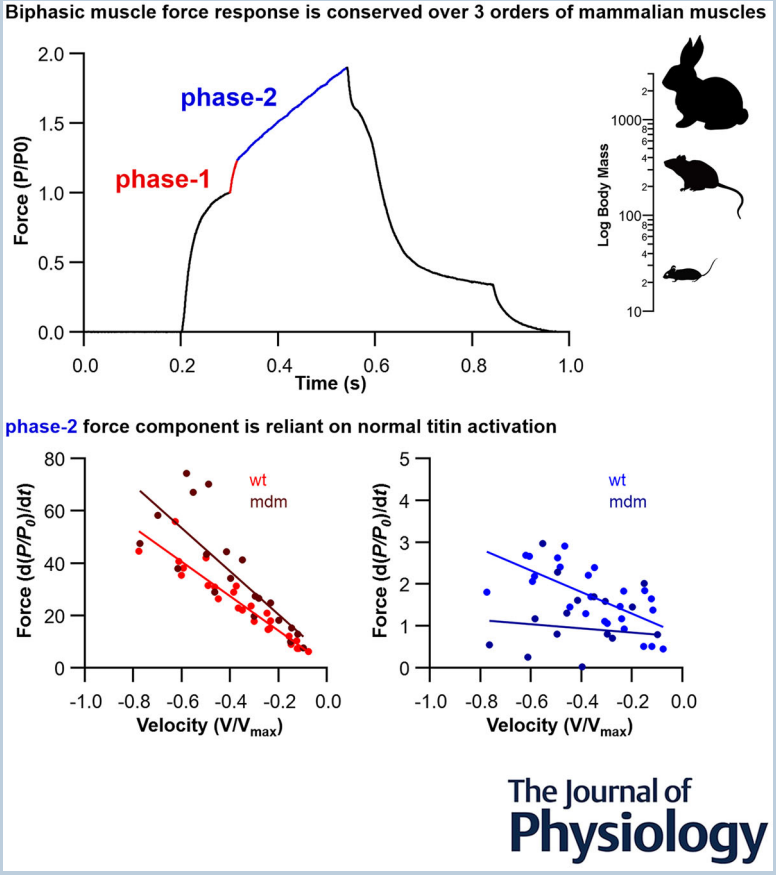

Roger W. P. Kissane is currently a post-doctoral research fellow at the University of Liverpool. His PhD at the University of Leeds focused on the regulation of skeletal muscle microvascular composition in response to distinct mechanotransductive stimuli. He then undertook a research project exploring the therapeutic potential of neuromodulation on the recovery of locomotor function following severe spinal cord injury. His current work is characterising the *in vivo* kinematics, kinetics and physiology of mastication.

DOI: 10.1113/JP285549

Abstract Skeletal muscle has a broad range of biomechanical functions, including power generation and energy absorption. These roles are underpinned by the force–velocity relationship, which comprises two distinct components: a concentric and an eccentric force–velocity relationship. The concentric component has been extensively studied across a wide range of muscles with different muscle properties. However, to date, little progress has been made in accurately characterising the eccentric force–velocity relationship in mammalian muscle with varying muscle properties. Consequently, mathematical models of this muscle behaviour are based on a poorly understood phenomenon. Here, we present a comprehensive assessment of the concentric force–velocity and eccentric force–velocity relationships of four mammalian muscles (soleus, extensor digitorum longus, diaphragm and digastric) with varying biomechanical functions, spanning three orders of magnitude in body mass (mouse, rat and rabbits). The force–velocity relationship was characterised using a hyperbolic-linear equation for the concentric component a hyperbolic equation for the eccentric component, at the same time as measuring the rate of force development in the two phases of force development in relation to eccentric lengthening velocity. We demonstrate that, despite differences in the curvature and plateau height of the eccentric force–velocity relationship, the rates of relative force development were consistent for the two phases of the force–time response during iso-velocity lengthening ramps, in relation to lengthening velocity, in the four muscles studied. Our data support the hypothesis that this relationship depends on cross-bridge and titin activation. Hill-type musculoskeletal models of the eccentric force–velocity relationship for mammalian muscles should incorporate this biphasic force response.

(Received 4 September 2023; accepted after revision 1 February 2024; first published online 24 February 2024)
Corresponding author R. W. P. Kissane: Department of Musculoskeletal & Ageing Science, University of Liverpool, The William Henry Duncan Building, 6 West Derby Street, Liverpool, L7 8TX, UK. Email: r.kissane@liverpool.ac.uk
G. N. Askew: School of Biomedical Sciences, University of Leeds, UK. Email: g.n.askew@leeds.ac.uk

Abstract figure legend The biphasic force response seen during active muscle lengthening is conserved over three orders of magnitude of mammalian skeletal muscle mass. Using mice with a small deletion in titin (mdm), we show that the phase-2 portion (blue) of the biphasic force profile in response to muscle lengthening is reliant on normal titin activation. The rate of force development during muscle stretch may be a more reliable way to describe the forces experienced during eccentric muscle contractions compared to the traditional hyperbolic curve fitting, and functions as a novel predictor of force–velocity characteristics that may be used to better inform musculoskeletal models and assess pathophysiological remodelling.

Key points

- The capacity of skeletal muscle to generate mechanical work and absorb energy is underpinned by the force–velocity relationship.
- Despite identification of the lengthening (eccentric) force–velocity relationship over 80 years ago, no comprehensive study has been undertaken to characterise this relationship in skeletal muscle.
- We show that the biphasic force response seen during active muscle lengthening is conserved over three orders of magnitude of mammalian skeletal muscle mass.
- Using mice with a small deletion in titin, we show that part of this biphasic force profile in response to muscle lengthening is reliant on normal titin activation.
- The rate of force development during muscle stretch may be a more reliable way to describe the forces experienced during eccentric muscle contractions compared to the traditional hyperbolic curve fitting, and functions as a novel predictor of force–velocity characteristics that may be used to better inform hill-type musculoskeletal models and assess pathophysiological remodelling.

Introduction

Skeletal muscles have a broad range of biomechanical functions: muscles may generate force during shortening to generate mechanical work, functioning as a motor; other muscles may primarily be active during muscle lengthening, dissipating mechanical energy and functioning as a brake; and others may operate as tension

struts, generating force without undergoing any change in length (Azizi, 2014; Charles et al., 2022; Kissane et al., 2022; Lai et al., 2019; Usherwood, 2022). The capacity of skeletal muscle to generate and absorb mechanical work and power is underpinned by the force–velocity relationship (Askew, 2023). This relationship comprises two distinct components: a shortening (or concentric) force–velocity relationship (Hill, 1938) and a lengthening (or eccentric) force–velocity relationship (Edman et al., 1978).

Although the shortening force–velocity relationship has been extensively investigated across a range of phenotypically distinct muscles (Askew & Marsh, 1997; Barclay, 1996), scaling relationships (Pellegrino et al., 2003) and even in response to pathophysiological remodelling (Espino-Gonzalez et al., 2021; Warren et al., 2020), the lengthening force–velocity relationship has been comparably less well studied (Mendoza et al., 2023). Despite identification of the relationship over 80 years ago (Katz, 1939), no comprehensive study has been undertaken to characterise this relationship in skeletal muscle. Previous studies have used different methodological approaches. Some studies have used isovelocity (velocity clamped) contractions, whereas others have used isotonic (force clamped) contractions, which yield different force profiles and consequently different force–velocity relationships (Woledge et al., 1985). Some investigations have used rather small sample sizes (Joyce et al., 1969), or been completed at non-physiological temperatures (Alcazar et al., 2019; Edman, 1988; Lännergren, 1978) and carried out using a variety of species (mammalian, amphibians and crustacean), rendering much of the data available difficult to collate to obtain a generalised understanding of muscle functional behaviour (Alcazar et al., 2019). This is problematic because skeletal muscles function eccentrically across a number of locomotor behaviours such as walking (Gillis et al., 2005; Lai et al., 2019), flying (Askew & Marsh, 2001) and feeding (Mayerl et al., 2021). Our limited understanding of this complex behaviour means that estimates of whole motor systems through Hill-type musculoskeletal models are potentially misrepresentative of their true function. Additionally, these principles form the basis of our understanding and investigation of motor control strategies, where, for example, muscle spindles are assumed to be sensitive to not only muscle lengthening velocity, but also force generation (Blum et al., 2017; Blum et al., 2020; Kissane et al., 2022, 2023).

The lack of extensive progress in characterising the eccentric force–velocity relationship is perhaps partly a result of the complex nature of the muscle force response to active lengthening. It has long been known that muscles undergoing active lengthening produce a dynamic biphasic force response (Herzog, 2014; Herzog et al., 2016; Joyce et al., 1969; Krylow & Sandercock, 1997; Pinniger et al., 2006; Weidner et al., 2022). This biphasic force response (see Appendix, Fig. A1) comprises a phase of rapid force development (phase-1) and a phase of slow force development (phase-2). This complex phenomenon is thought to arise from two distinct mechanical processes. First, the initial rapid phase-1 response is hypothesised to arise from elevated strain of attached cross-bridges, after which the detachment of myosin heads leads to the transition into the shallower phase-2 force response (Tomalka, 2023; Tomalka et al., 2020, 2021; Weidner et al., 2022). The phase-2 force response is assumed to be linked to increased strain of non-cross-bridge, parallel elastic elements (Ramsey et al., 2010; Tomalka, 2023). Little is known about the rate of force development in these two phases in relation to lengthening velocity, or how or whether this relationship differs between muscles of distinctive phenotypes, or as a result of scaling in relation to body mass. Hence, we have set out to undertake the most comprehensive assessment of eccentric muscle contractile properties to date.

First, we investigated the eccentric response of the phenotypically distinct fast extensor digitorum longus (EDL) and slow soleus (SOL) muscles from the mouse. Despite the comprehensive characterisation of the distinct shortening force–velocity (concentric) properties of these muscles, little is known of the eccentric force–velocity relationship of these two muscles and, specifically, whether there is variation in the rate of force development during phase-1 and phase-2. When skinned muscle fibres of differing fibre phenotype were actively lengthened, they produced comparable steady-state forces and power output (Linari et al., 2004). To achieve this, slow fibres recruit more myosin head attachments, to make up for the difference in initial isometric force (Linari et al., 2004). It is assumed that the force enhancement contributed to by contractile elements is greater in the SOL than in the EDL, and that the non-contractile contribution to force enhancement is greater in the EDL than the SOL (Ramsey et al., 2010). These mechanistic differences in active lengthening are considered to lead to differences in the rate of force development during stretch (Hessel & Nishikawa, 2017) between phenotypically different muscles. Therefore, we hypothesise that, similar to phenotypically distinct skinned fibres, there may exist differences in the classical force–velocity relationship between the SOL and EDL (Linari et al., 2004). In addition, we expect that, given the proposed differences in contribution of the contractile and non-contractile elements (Prado et al., 2005) to the SOL and EDL during eccentric contractions, both the rates of force development during phase-1 and phase-2 will differ between the two muscles.

In addition to the EDL and SOL from the mouse, we also investigated the eccentric contractile properties of the diaphragm (DIA) muscle from the rat and the digastric

(DIG) muscle from the rabbit, extending the range in body mass of the species studied to cover three orders of magnitude. These anatomically and functionally diverse examples of mammalian muscle provide a unique opportunity to test whether this biomechanical phenomenon is conserved between species. We hypothesise that the biphasic force development profile will be conserved between these mammalian species, and that they may present with comparable rates of force enhancement across a range of lengthening velocities.

Finally, as mentioned previously, the rapid phase-1 force development profile is assumed to be the response to elevated strain of attached cross-bridges (Tomalka, 2023; Tomalka et al., 2020, 2021; Weidner et al., 2022), with the phase-2 force response assumed to be linked to increased strain of non-cross-bridge parallel elastic elements (De Ruiter et al., 2000; Ramsey et al., 2010; Tomalka, 2023). Recent work has shown that titin plays an important role in both passive and active muscle properties, contributing to force enhancement and depression during lengthening and shortening contractions (Tahir et al., 2020). It is therefore plausible that titin plays an important role in the rate of force development during eccentric contractions. Therefore, we have utilised the muscular dystrophy with myositis (mdm) mouse model (Powers et al., 2016; Tahir et al., 2020) with impaired titin activation to investigate the potential contribution of titin to biphasic force development response. It has previously been shown that cross-bridge kinetics are relatively unaffected in mice with mdm (Tahir et al., 2020); therefore, we hypothesise that the impaired titin function in the mdm mice will not affect the phase-1 portion of the eccentric force response. However, it probably directly impairs the phase-2 portion of the eccentric force response, given that it has been associated mechanism with non-cross-bridge elastic elements.

In summary, we show that the dynamic two-phase force development response of skeletal muscle to active lengthening has a strong, velocity-dependent relationship across all four mammalian muscles. We provide evidence for a novel predictor of force–velocity characteristics, specifically, the rate of force developed during eccentric lengthening, which may be used to better inform Hill-type musculoskeletal models and assess pathophysiological remodelling. Our data also show that the second-phase shallow rate of force development during eccentric contractions is dependent on normal titin activation, but the rapid (phase-1) response is not.

Methods

Ethical approval

All experimental procedures were performed in accordance with the UK animal scientific procedures act (1986) and approved by the University of Leeds Animal Welfare (PPL: PA1BA29DF) and Ethical Review Committee. This work conforms to the ethical requirements outlined by the journal and is presented in accordance with guidelines for animal work (Grundy, 2015; Percie du Sert et al., 2020).

Animals

Twenty-one in-house male C57B6 mice (25.06 ± 1.90 g), five in-house male Wistar rats (254 ± 10 g) and eight male New Zealand white rabbits (Envigo, Indianapolis, IN, USA) (2638 ± 85 g) were used in the present study. Animals were housed under a 12:12 h light/dark photocycle at 21°C and had *ad libitum* access to food and water.

Ex vivo muscle preparation

Both mice and rats were culled using approved schedule 1 methods. The hindlimb of the mouse and the whole rat DIA were transferred to chilled (4°C), oxygenated (95% O_2, 5% CO_2) Krebs–Henseleit solution (in mmol L^{-1}: 117 NaCl, 4.7 KCl, 2.5 $CaCl_2$, 1.2 $MgSO_4$, 24.8 $NaHCO_3$, 1.2 KH_2PO_4 and 11.1 glucose) (Burton, 1975). The whole SOL and EDL were dissected free and aluminium foil clips were attached to the proximal and distal ends of the muscles, with no free tendon left in series (Askew & Marsh, 1997). The rat DIA was pinned out at approximately resting length, and a medial section of the costal diaphragm (width 4−5 mm) was dissected maintaining a rib at the proximal end, and a stainless-steel ring was sutured to the central tendon (Warren et al., 2020). The SOL, EDL and DIA were suspended vertically in a flow-through Perspex chamber filled with circulating, oxygenated Krebs–Henseleit solution at 37 ± 0.5°C. Muscles were attached to an ergometer (series 300B-LR; Aurora Scientific Inc., London, ON, Canada) via a lightweight stainless-steel rod and muscle length was altered using a micromanipulator. Muscles were left for 30 min to thermo-equilibrate and recover from the dissection. Parallel platinum electrodes were placed inside the chamber on either side of and parallel to the muscle.

In situ muscle preparation

Rabbits were anaesthetised with a subcutaneous injection of ketamine (Ketavet; Zoetis, Parsippany-Troy Hills, NJ, USA; 50 mg kg^{-1}) and xylazine (Rompun; Bayer, Leverkusen, Germany; 5 mg kg^{-1}). Following confirmation of anaesthetic plane, an I.V. canula was implanted to deliver a maintenance dose of ketamine and xylazine throughout the experiment. The DIG muscle was

exposed via an incision running the length of the dorsal aspect of the jaw. A 3 mm hole was drilled through the mandible and a custom 3-D printed mould was screwed to the bone and attached to a custom rig to allow for muscle length to be changed. The distal end of the DIG was sutured to a stainless-steel loop with silk suture (3-0; LOOK Braided suture, Surgical Specialties, Westwood, Massachusetts, USA) and hooked onto the ergometer (305B-LR; Aurora Scientific Inc., Aurora, ON, Canada). Parallel platinum wires (0.4 mm in diameter) were implanted into the DIG muscle using a 25-gauge needle and sutured into place. The rabbit was left for 30 min to recover from electrode implantation, prior to beginning the muscle mechanical experiments. Throughout the experiment the rabbit's body temperature was maintained at 37°C (Animal Temperature Controller 2000; World Precision Instruments Sarasota, FL, USA) and the muscle was regularly irrigated with warmed (37°C) saline. Following completion of the experiment, rabbits were culled with an overdose of pentobarbital.

Isometric muscle properties

All muscles were subjected to a series of isometric twitches (supramaximal stimulus of 0.2 ms pulse) and muscle lengths were incrementally increased to find the optimal length of force generation (L_0). Maximal isometric tetanic force (P_0) at L_0 was determined using a train of stimuli delivered at 150 Hz for 250 ms for the SOL, at 250 Hz for 200 ms for the EDL, at 200 Hz for 200 ms for the DIA and 200 Hz for 300 ms for the DIG. Data were sampled at 2 kHz during isometric twitch kinetics. From these data the twitch-rise times and maximal isometric tetanic stress were calculated.

Force–velocity characteristics

The concentric force–velocity relationship of the SOL, EDL, DIA and DIG were determined using a series of isotonic afterload contractions across a range of forces (5%–80% of P_0) (Fig. 1*A*; see also Appendix, Figs A1 and A2) (Kissane et al., 2018), with data sampled at 2 kHz. Velocity and force were measured as the muscle shortened across L_0 (Fig. 1*A*; see also Appendix Figs A1 and A2) and the force–velocity relationship was determined by fitting a hyperbolic-linear function (Marsh & Bennett, 1986) to the data (Eqn 1). The maximal shortening velocity at zero force (V_{max}), expressed relative to fibre length (FL) for the SOL, EDL, DIA and DIG, was calculated. Peak instantaneous isotonic power ($\dot{W}_{max}$) and the power

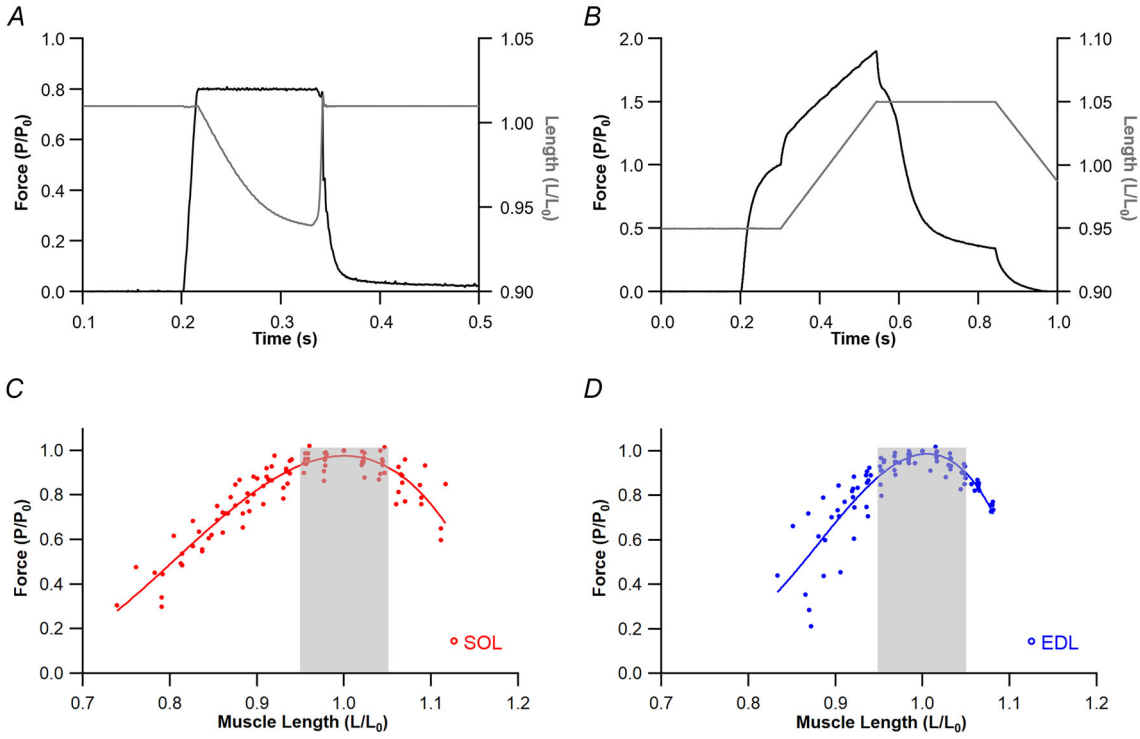

Figure 1. Muscle mechanical procedure
Isotonic muscle shortening (*A*) and isovelocity muscle lengthening (*B*) protocols. Complete force-length relationships for the soleus (*C*) and extensor digitorum longus (*D*) with the shaded region highlighting the region with which isovelocity lengthening was conducted.

ratio ($\dot{W}_{max}/P_0V_{max}$), were also determined from the fitted force–velocity relationship.

$$V = \frac{B\left(1-\frac{P}{P_0}\right)}{\left(A+\frac{P}{P_0}\right)+C\left(1-\frac{P}{P_0}\right)} \quad (1)$$

where P/P_0 is relative force and A, B and C are coefficients. The lengthening force–velocity relationship of the SOL, EDL, DIA and DIG was determined using isovelocity lengthening ramps (Fig. 1*B*). The SOL, EDL, DIA and DIG were lengthened by 2, 1, 3 and 2 mm, respectively, symmetrically spanning L_0 (Fig. 1*C* and *D*). Force and velocity were averaged across L_0 (selecting ±1% muscle length) and used to plot the eccentric force velocity relationship. Muscles were lengthened at velocities up 60% of V_{max}, and the data was sampled at 5 kHz. The lengthening force–velocity relationship was fit with a hyperbolic function (Alcazar et al., 2019) (Eqn 2). Coefficients D and E were derived which describe the plateau height (D) and curvature (E) of the relationship (see Appendix, Fig. A3).

$$P = \frac{E-DV-2V}{E-V} \quad (2)$$

Titin mutant mice

Raw eccentric ramp data were taken from Tahir et al. (2020). Briefly, muscular dystrophy with myositis (mdm) and wild-type (WT) soleus muscles were subjected to eccentric ramps over a 200 ms period, varying the muscle amplitude from +10% to −10%, +8% to −8%, +6% to −6%, +4% to −4%, +2% to −2% of L_0, covering a range of velocities from 0.2 to 1 mL s^{-1}. Raw data from these experiments were used to calculate the rates of force development in phase-1 and phase-2 during the eccentric ramp.

Statistical analysis

All data processing and figures were plot using Igor Pro 8 (WaveMetrics, Portland, OR, USA). One-way analysis of variance (ANOVA) was completed using SPSS, version 28 (IBM Corp., Armonk, NY, USA), where significance was detected *post hoc* comparisons were made using the Bonferroni correction and the threshold for statistical significance was set to $P < 0.05$. Repeated measures correlations (Bakdash & Marusich, 2017) were undertaken using CRAN R (https://cran.r-project.org/web/packages/rmcorr) in R software (R Foundation, Vienna, Austria). Least-squares regression slopes between the rate of force development and lengthening velocity were determined for pooled data to determine whether significant differences existed between the slopes when accounting for passive force (Kissane et al., 2019; McFarlane et al., 2016). All data are presented as the mean ± SD.

Results

Phenotypically distinct muscles from the mouse have distinct eccentric force–velocity characteristics

The shortening force–velocity characteristics for the mouse EDL and SOL have been comprehensively described in the literature (Askew & Marsh, 1997; Askew et al., 1997; Barclay, 1996; Luff, 1981). Our data presented here (Fig. 2*A* and *D* and Table 1) show the EDL to have a significantly greater V_{max} (14.1 ± 1.8 FL s^{-1} *vs.* 7.0 ± 0.6 FL s^{-1}, $t_{19} = -12.967$, $P < 0.001$), a higher power ratio (0.128 ± 0.014 *vs.* 0.089 ± 0.008, $t_{19} = -7.515$, $P < 0.001$) and greater $\dot{W}_{max}$ (402.6 ± 108.2 W kg^{-1} *vs.* 120.0 ± 32.6 W kg^{-1}, $t_{19} = -8.551$, $P < 0.001$) compared to the SOL. These values are comparable to previously published values (Askew & Marsh, 1997; Holt & Askew, 2012; Luff, 1981). In addition to the significantly different isometric twitch kinetics and isotonic shortening profiles (Table 1) the EDL and SOL present with significantly different eccentric force–velocity profiles (Fig. 2*A* and *D* and Table 2) with a significantly lower plateau (D coefficient; −0.500 ± 0.039 *vs.* −0.313 ± 0.063, $t_{19} = 8.082$, $P < 0.001$) and lower degree of curvature of this relationship (E coefficient; 0.571 ± 0.313 *vs.* 0.289 ± 0.117, $t_{19} = -2.788$, $P = 0.012$) in EDL compared to SOL.

As previously mentioned, during the isovelocity ramp the force response presents with a biphasic profile (Herzog, 2014; Herzog et al., 2016; Joyce et al., 1969; Krylow & Sandercock, 1997; Weidner et al., 2022) (Fig. 1*B*; see also Appendix Figs A1 and A2), comprising a phase of rapid force development (phase-1) and a phase of slow force development (phase-2). Looking specifically at the rate of force development during phase-2 as the eccentric ramp crosses L_0, there is a significantly strong relationship between the rate of force development and the absolute velocity of lengthening for the EDL [r_{rm} (24) = −0.9746, 95% confidence interval (CI) = −0.9887 to −0.9433; $P < 0.001$] (Fig. 2*B*) and for the SOL [r_{rm} (37) = −0.9750, 95% CI = −0.9869 to −0.9525; $P < 0.001$] (Fig. 2*B*) with the rate of change of force increasing with increasing velocity of stretch. This significantly strong relationship is also evident during the phase of rapid force development (i.e. phase-1) (Fig. 1*B*; see also Appendix Figs A1 and A2) in both the EDL [r_{rm} (24) = −0.9794, 95% CI = −0.9909 to −0.9540; $P < 0.001$] (Fig. 2*C*) and SOL [r_{rm} (37) = −0.9907, 95% CI = −0.9951 to −0.9821; $P < 0.001$] (Fig. 2*C*) muscles, with the rate of change of force increasing with increasing velocity of stretch. When eccentric velocity is normalised to the muscle-specific V_{max}, these significantly strong relationships remain (Fig. 2*E* and *F*).

Table 1. Isometric and isotonic properties of the soleus (SOL), extensor digitorum longus (EDL), diaphragm (DIA) and digastric (DIG) muscle

	SOL	EDL	DIA	DIG	*F*	*P* value
Isometric stress (kN m^{-2})	203.2 ± 46†	236.4 ± 51.1†	185.3 ± 16.0†	383.7 ± 76.6$^{*\,\S\,\#}$	18.39	<0.001
Twitch rise time (ms)	17.2 ± 1.8$^{\S\,\dagger\,\#}$	8.0 ± 0.6$^{*\,\dagger\,\#}$	22.3 ± 2.1$^{*\,\S\,\dagger}$	36.5 ± 4.4$^{*\,\S\,\#}$	209.256	<0.001
Half-relaxation time (ms)	21.3 ± 2.4$^{\S\,\dagger\,\#}$	9.4 ± 1.8$^{*\,\dagger\,\#}$	26.3 ± 1.9$^{*\,\S\,\dagger}$	30.4 ± 2.4$^{*\,\S\,\#}$	158.956	<0.001
V_{max}	7.01 ± 0.6$^{\S\,\dagger\,\#}$	14.14 ± 1.77$^{*\,\dagger\,\#}$	10.18 ± 1.58$^{*\,\S}$	11.09 ± 2.13$^{*\,\S}$	35.306	<0.001
$\dot{W}_{max}$	120.0 ± 32.6§	402.6 ± 108.2*	160.8 ± 23.3§	142.4 ± 29.6§	35.101	<0.001
P/P_0 at maximal power	0.30 ± 0.02§	0.39 ± 0.02*	0.33 ± 0.01$^{\S\,\dagger}$	0.38 ± 0.05$^{*\,\#}$	20.505	<0.001
V/V_{max} at maximum power	2.05 ± 0.19$^{\S\,\dagger\,\#}$	4.64 ± 0.63$^{*\,\dagger\,\#}$	2.81 ± 0.25$^{*\,\S\,\dagger}$	0.98 ± 0.13$^{*\,\S\,\#}$	121.536	<0.001
Power ratio	0.089 ± 0.008§	0.128 ± 0.013$^{*\,\dagger\,\#}$	0.091 ± 0.006§	0.104 ± 0.023§	16.623	<0.001
V/V_{max}	2.05 ± 0.19	3.08 ± 0.46	3.61 ± 0.25	3.47 ± 0.34	2.852	0.055

V_{max}, maximum shortening velocity; W_{max}, maximum isotonic power. Data are the mean ± SD.
$^{*}P < 0.05$ *vs.* SOL.
$^{\S}P < 0.05$ *vs.* EDL.
$^{\#}P < 0.05$ *vs.* DIA.
$^{\dagger}P < 0.05$ *vs.* DIG.

The rate of force development during eccentric contractions scales across muscles from species covering three orders of magnitude in body mass

In addition to the EDL and SOL from the mouse, we have also investigated the eccentric contractile properties of the DIA muscle from the rat and the DIG muscle from the rabbit, extending the range in body mass of the species studied to cover three orders of magnitude (Fig. 3*A*). Not only are these muscles significantly different in mass (ANOVA: $F_{3,28} = 349.755$, $P < 0.001$) (Fig. 3*B*), they are also phenotypically distinct (Askew & Marsh, 1997; Warren et al., 2020) (Fig. 3*C*) and are anatomically divergent with a range of relative fibre-to-muscle lengths

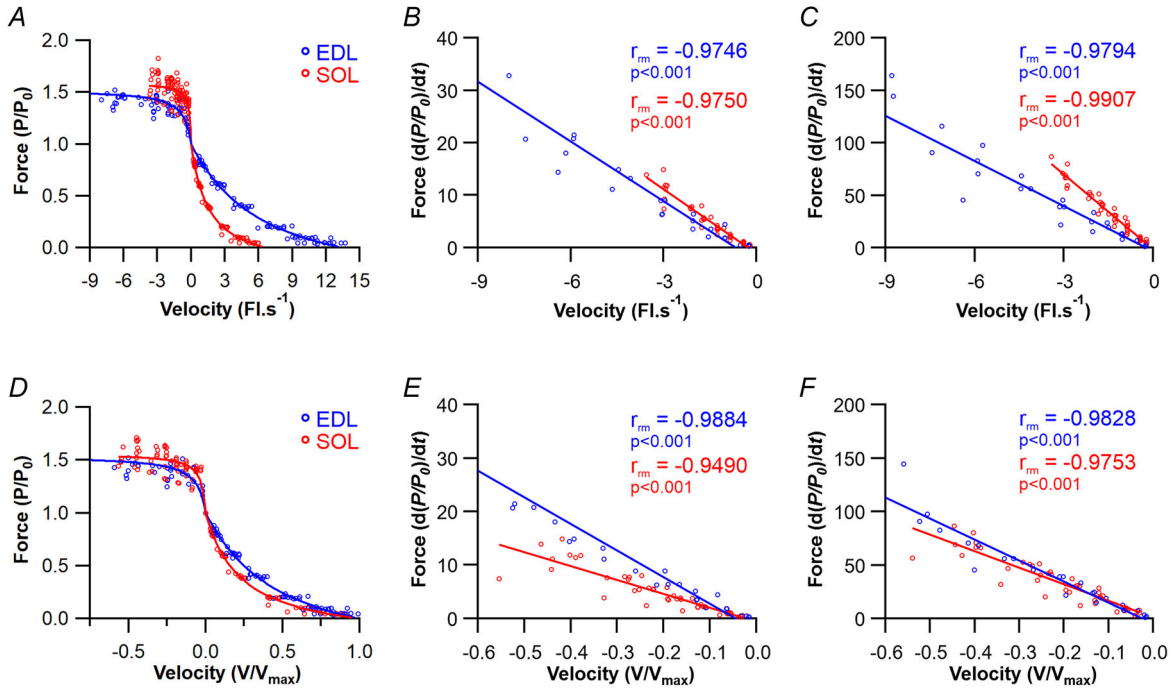

Figure 2. Muscle force–velocity characteristics of two phenotypically distinct muscles
A, absolute force velocity relationship. Rate of force development as a function of lengthening velocity across the phase-2 (*B*) and phase-1 (*C*). *D*, normalised force velocity relationship. Rate of force development as a function of normalised lengthening velocity across the phase-2 (*E*) and phase-1 (*F*).

Table 2. Coefficients for the force–velocity relationship fit to the soleus (SOL), extensor digitorum longus (EDL), diaphragm (DIA) and digastric (DIG) muscle

	SOL	EDL	DIA	DIG	*F*	*P* value
A	0.244 ± 0.130	0.396 ± 0.295	0.190 ± 0.036	0.172 ± 0.069	2.355	0.093
B	1.81 ± 1.18	5.56 ± 5.39†	1.75 ± 0.13	0.511 ± 0.258§	3.843	0.020
C	−0.157 ± 1.045	1.547 ± 3.019	0.779 ± 0.377	0.657 ± 0.358	1.276	0.302
D	−0.313 ± 0.063$^{\S\ \#}$	−0.500 ± 0.039$^{*\ \dagger\ \#}$	−0.0872 ± 0.0485$^{*\ \S}$	−0.190 ± 0.216§	24.462	<0.001
E	0.289 ± 0.117†	0.571 ± 0.313	0.231 ± 0.051	0.960 ± 1.000*	3.481	0.029

Coefficients *A*, *B* and *C* correspond to values for the Marsh and Bennett (1986) hyperbolic linear equation fit for the concentric portion of the force–velocity relationship presented in Equation (1), whereas *D* and *E* correspond to value fit for the rearranged hyperbolic equation from Alcazar et al. (2019) to fit the eccentric portion of the force–velocity relationship, displayed in Eqn (2). Data are the mean ± SD.
$^{*}P < 0.05$ *vs.* SOL.
$^{\S}P < 0.05$ *vs.* EDL.
$^{\#}P < 0.05$ *vs.* DIA.
$^{\dagger}P < 0.05$ *vs.* DIG.

(Altringham & Young, 1991; Askew & Marsh, 1997; Dantuma & Weijs, 1980) (Fig. 3*D*), and body mass normalised fibre length and physiological cross-sectional area (Fig. 3*E*). Therefore, these anatomically and functionally diverse examples of mammalian muscle provide a unique opportunity to examine the potential differences in eccentric muscle properties, should they exist. The isometric properties of these four muscles

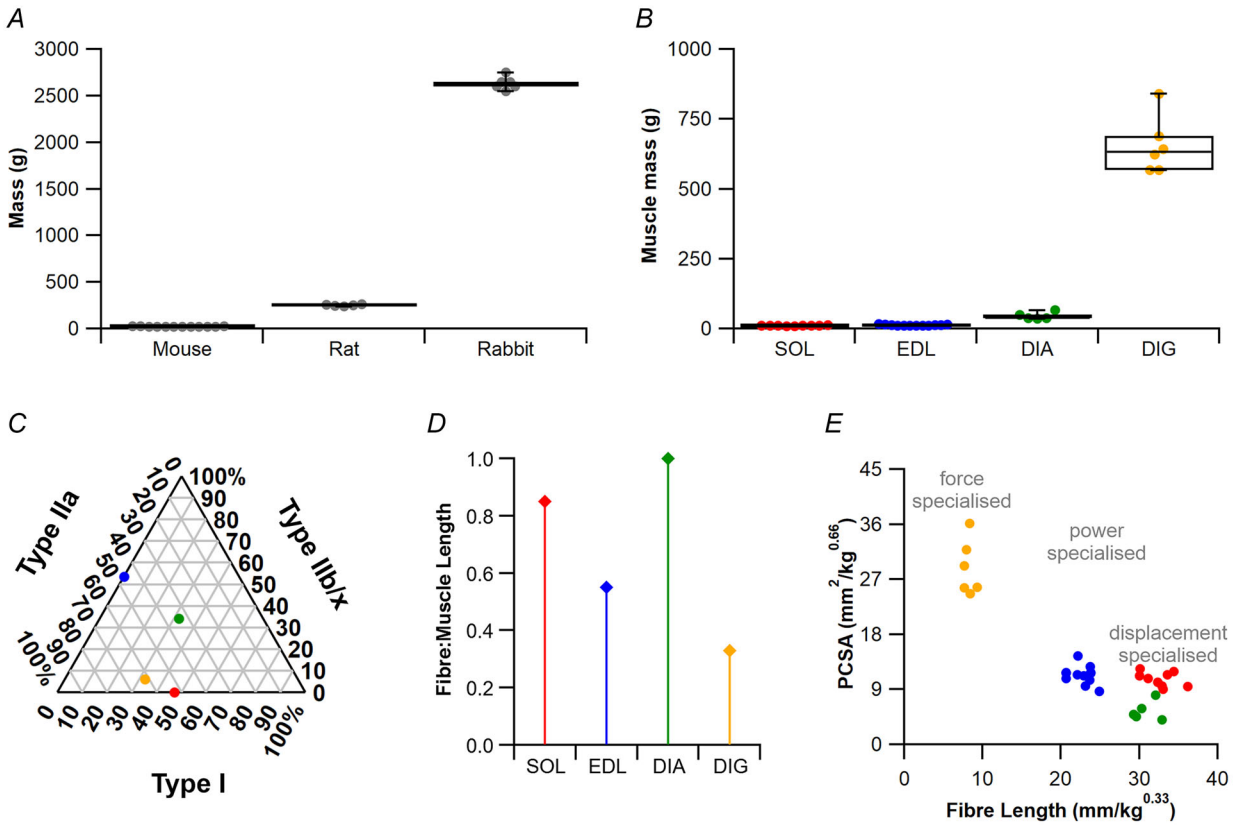

Figure 3. Comparative muscle architecture across mammalian muscles
Here, we have used species that range three order of magnitude in body mass (*A*) and muscle mass (*B*). These muscles have distinctive muscle fibre phenotypes (*C*), relative muscle fibre to whole muscle lengths (*D*) and are architecturally distinct in their muscle morphology (*E*).

were significantly different in their twitch-rise time (ANOVA: $F_{3,28} = 209.256$, $P < 0.001$) (Table 1) and half-relaxation time (ANOVA: $F_{3,28} = 158.956$, $P < 0.001$) (Table 1). Moreover, the muscle shortening force–velocity properties of these four muscles were significantly different (Table 1) with significantly different maximum shortening velocities (ANOVA: $F_{3,28} = 35.306$, $P < 0.001$) (Fig. 4*A*, *D*, *G* and *J*, and Table 1), $\dot{W}_{max}$ (ANOVA: $F_{3,28} = 35.101$, $P < 0.001$) (Fig. 4*A*, *D*, *G* and *J*, and Table 1) and power ratios (ANOVA: $F_{3,28} = 16.623$, $P < 0.001$) (Fig. 4*A*, *D*, *G* and *J*, and Table 1).

In addition to the distinct muscle shortening properties, there were significant differences in the eccentric plateau height coefficient (ANOVA: $F_{3,27} = 24.462$, $P < 0.001$) (Fig. 4*A*, *D*, *G* and *J*, and Table 2) and curvature coefficient (ANOVA: $F_{3,27} = 3.481$, $P = 0.029$) (Fig. 4*A*, *D*, *G* and *J*, and Table 2) across the four muscles. As found in the mouse SOL and EDL, the rat DIA (Fig. 4*G*–*I*) and the rabbit DIG (Fig. 4*J*–*L*) muscle also exhibited a significantly strong correlation between the rate of change of relative force with respect to time and stretch velocity during both phase-1 [DIA: r_{rm} (39) = −0.9837, 95% CI = −0.9913 to −0.9694; $P < 0.001$; DIG: r_{rm} (11) = −0.9567, 95% CI = −0.9873 to −0.8578; $P < 0.001$] and phase-2 [DIA: r_{rm} (39) = −0.9781, 95% CI = −0.9884 to −0.9591; $P < 0.001$; DIG: r_{rm} (11) = −0.9471, 95% CI = −0.9844 to −0.8284; $P < 0.001$], respectively. Moreover, pooling data from all four muscles shows that there is a significantly conserved absolute fibre lengthening velocity-dependant relationship with the rate of force development across the two phases of mammalian muscle [phase-1: r_{rm} (114) = −0.9663, 95% CI = −0.9765 to −0.9516; $P < 0.001$; Phase-2: r_{rm} (114) = −0.9167, 95% CI = −0.9417 to −0.8818; $P < 0.001$] (Fig. 5*A*) and normalised fibre lengthening velocity [phase-1: r_{rm} (114) = −0.9631, 95% CI = −0.9744 to −0.9471; $P < 0.001$; phase-2: r_{rm} (114) = −0.9147, 95% CI = −0.9402 to −0.8790; $P < 0.001$] (Fig. 5*B*). As well as the significantly conserved phase-1 and phase-2 rates of force development in relation to stretch velocity, the transition point between the two phases is significantly correlated with lengthening velocity across all four muscles (Fig. 6*A*–*D*) and the pooled muscle data (Fig. 6*E* and *F*), occurring at a higher P/P_0 with increasing velocity of stretch. Finally, the relationship between rate of force development and stretch velocity is robust regardless of force normalisation strategy, including normalisation to physiological cross-sectional area [phase-1: r_{rm} (114) = −0.9667, 95% CI = −0.9769 to −0.9522; $P < 0.001$; phase-2: r_{rm} (114) = −0.9079, 95% CI = −0.9354 to −0.8695; $P < 0.001$] (see Appendix Fig. A4), which may be of more translatable benefit to Hill-type musculoskeletal modellers (Charles et al., 2022; Kissane et al., 2022; Rajagopal et al., 2016).

The dynamic two-phase eccentric contraction response is not a function of passive muscle properties, but is dependent on titin activation

The passive muscle properties across all four muscles tested differed in relation to the active length-force relationship (Fig. 7*A*–*D* and *F*). The passive force at L_0 as a proportion of isometric twitch force was significantly different between the four muscles, ranging from 0.34 in SOL to 0.05 in DIG (ANOVA: $F_{3,23} = 11.724$, $P < 0.001$) (Fig. 7*E*). To examine the contribution of the passive muscle properties to the eccentric force–velocity relationship we performed active and passive eccentric ramps in the SOL, EDL and DIG (Fig. 8; see also Appendix Fig. A5). We show that, despite significantly different passive muscle properties (Fig. 7), it appears to have no significant contribution to the force profiles during lengthening of the DIG (see Appendix Fig. A5), SOL (Fig. 8) or EDL (Fig. 8) muscles. Briefly, individual active and active-minus-passive traces (see Appendix Fig. A5*A*–*C*) highlight the lack of contribution to the overall eccentric force profile and bear no significant contribution to the eccentric force–velocity relationship (see Appendix Fig. A5*G*). Despite the significantly different passive force at L_0 between the mouse SOL and EDL (Fig. 7*E*), there was no significant effect of these properties on the eccentric force–velocity relationship when accounting for passive force (Fig. 8*A*). Although the SOL and EDL have significantly different D (−0.287 ± 0.056 *vs.* −0.522 ± 0.031, $P < 0.001$) (Fig. 8*B* and Table 2) and E coefficients (0.265 ± 0.105 *vs.* 0.537 ± 0.135, $P = 0.005$) (Fig. 8*C* and Table 2), when accounting for the passive force (i.e. active force minus passive force), there was no significant change in the coefficient values in either muscle (Fig. 8*A*–*C*). Consequently there was no significant difference in the regression slopes for the relationship between rate force development and velocity of stretch in SOL ($t_{59} = 1.6765$, $P = 0.099$) (Fig. 8*D*) or EDL ($t_{48} = 1.5889$, $P = 0.119$) (Fig. 8*E*) when accounting for the passive force properties of the muscles.

Mice with impaired titin activation still have a relatively typical two-phase response to eccentric loading (Fig. 9*A*) and present with a significant relationship between the lengthening velocity and the rate of force development (Fig. 9*B* and *C*). The rate of force development during the first phase of the eccentric ramp was not significantly different between the wild-type (wt) and mdm mice ($t_{41} = 0.9057$, $P = 0.3704$) (Fig. 9*B*) and was not significantly different when accounting for passive muscle properties ($t_{41} = 1.1491$, $P = 0.2572$) (Fig. 9*D*). However, the second phase in the mdm muscle presents with a comparable significant relationship between the rate of force development and velocity of stretch (Fig. 9*C*), yet when accounting for the contribution of the passive

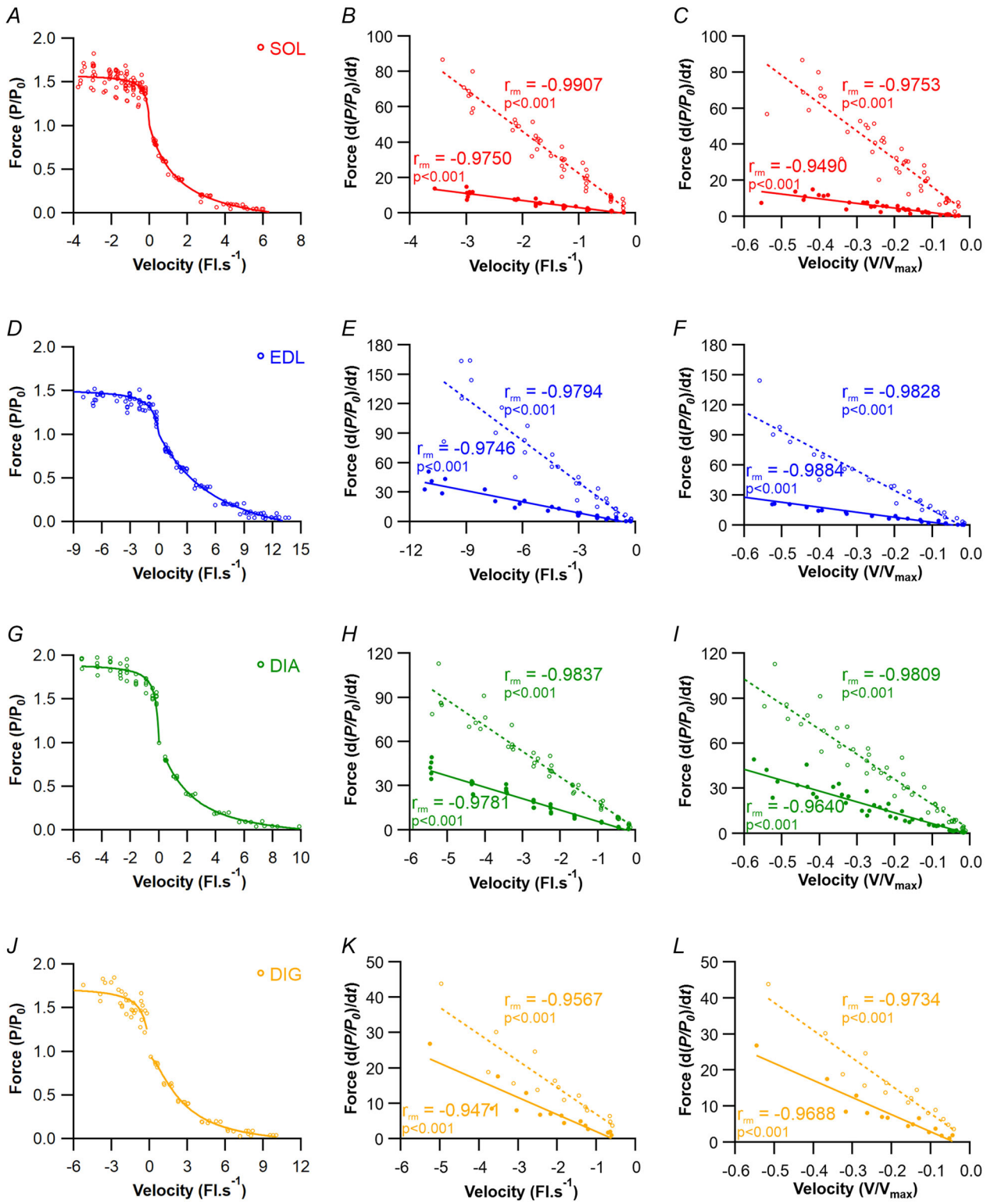

Figure 4. Force–velocity characteristics across four mammalian muscles
Absolute force velocity relationship (*A*, *D*, *G* and *J*), rate of force development as a function of absolute lengthening velocity across the first phase (dashed line) and second phase (continuous line) of the isovelocity relationship (*B*, *E*, *H* and *K*). Rate of force development as a function of normalised lengthening velocity across the first phase (dashed line) and second phase (continuous line) of the isovelocity relationship (*C*, *F*, *I* and *L*). Presented for the mouse soleus (*A*, *B* and *C*), mouse extensor digitorum longus (*D*, *E* and *F*), rat diaphragm (*G*, *H* and *I*) and rabbit digastric (*J*, *K* and *L*) muscles.

muscle properties this relationship is completely abolished (Fig. 9*E*). These data highlight the importance of titin activation on the rate of force development during eccentric muscle contractions.

Discussion

Despite the eccentric force–velocity relationship being generally described over 80 years ago, little progress has been made in determining whether muscle anatomical or intrinsic contractile properties underpin the shape of this relationship. This uncertainty presents a problem for modelling muscle behaviours that involve eccentric contractions, which is a common feature of many muscles that function during cyclical behaviours like locomotion (Askew & Marsh, 2001; Gillis & Biewener, 2001; Gillis et al., 2005; Mayerl et al., 2021; Roberts et al., 2007). Here, we present a comprehensive and robust data set of the

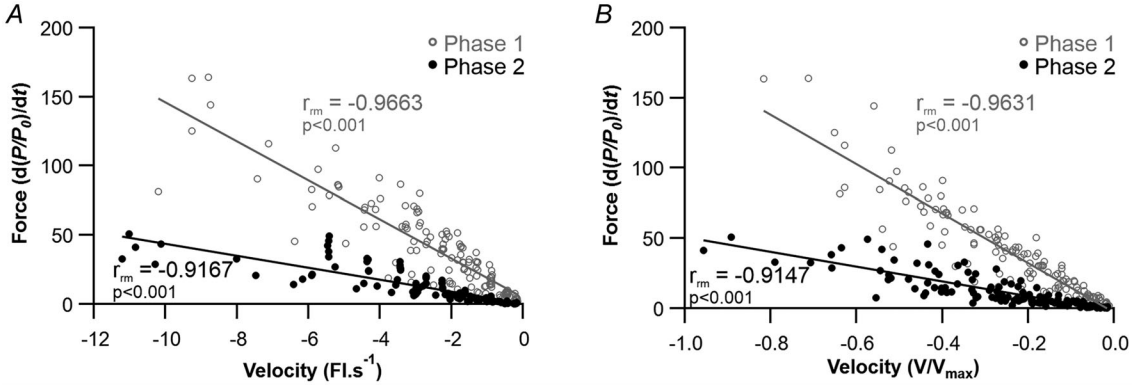

Figure 5. Pooled rate of force development as a function of P_0 during eccentric contractions
Pooled rate of force development as a function of absolute (fibre lengths per second) lengthening velocity (*A*) and normalised lengthening velocity (to maximum shortening velocity, V_{max}) (*B*) across phase-1 (unfilled grey) and phase-2 (filled black) of the isovelocity lengthening relationship.

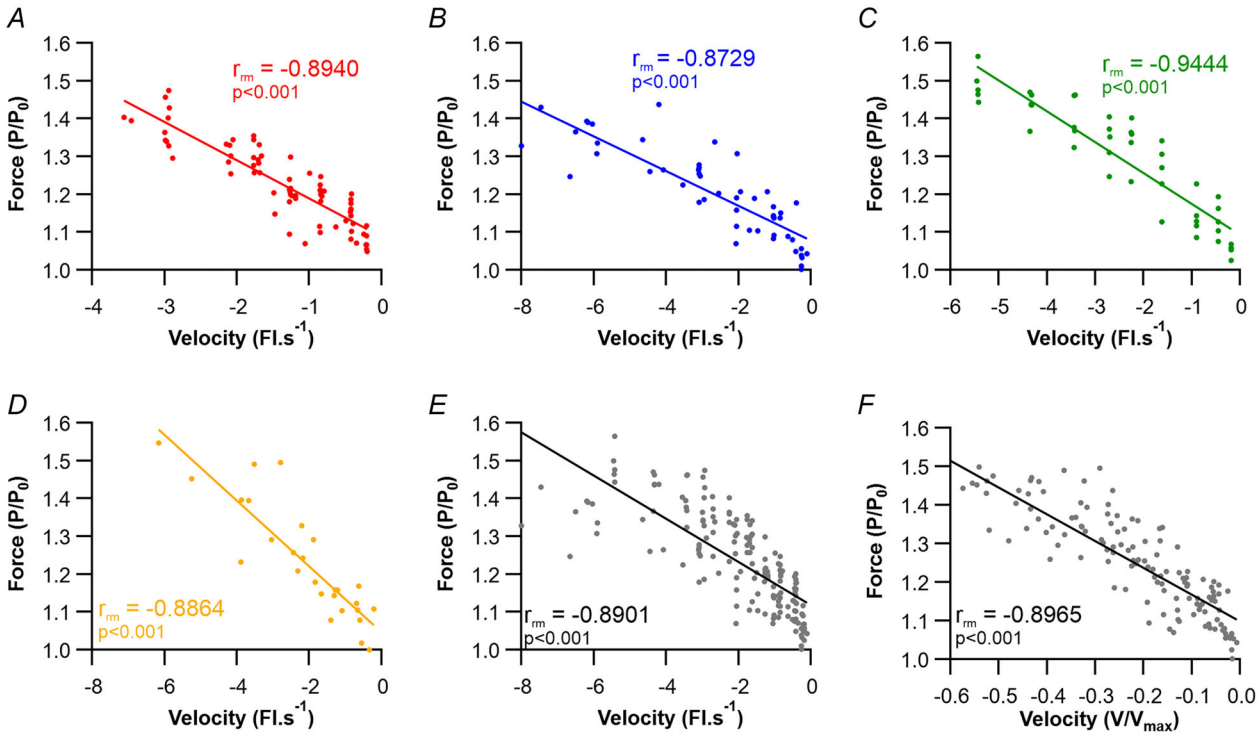

Figure 6. Relationship between the transition point between phase-1 and phase-2 of force development and lengthening velocity during the eccentric force–velocity relationship
The relationship between lengthening velocity and the transition from phase-1 to phase-2 for the SOL (*A*), EDL (*B*), DIA (*C*) and DIG (*D*) show significantly strong positive relationships. When pooled for absolute lengthening velocity (*E*) and normalised to V_{max} (*F*), this significant relationship is maintained.

complete (both concentric and eccentric) force–velocity relationships from mammalian muscles differing in both phenotype and muscle mass. We have shown that there are significant differences in the plateau height of the eccentric force–velocity relationship across this range of mammalian muscles. However, the more robust relationship may be that describing the rate of relative force development during eccentric muscle activation, with the relationship being highly conserved. Finally, we show that the rate of relative force development during phase-2 of eccentric force development is dependent on normal titin activation, whereas the initial first phase is not.

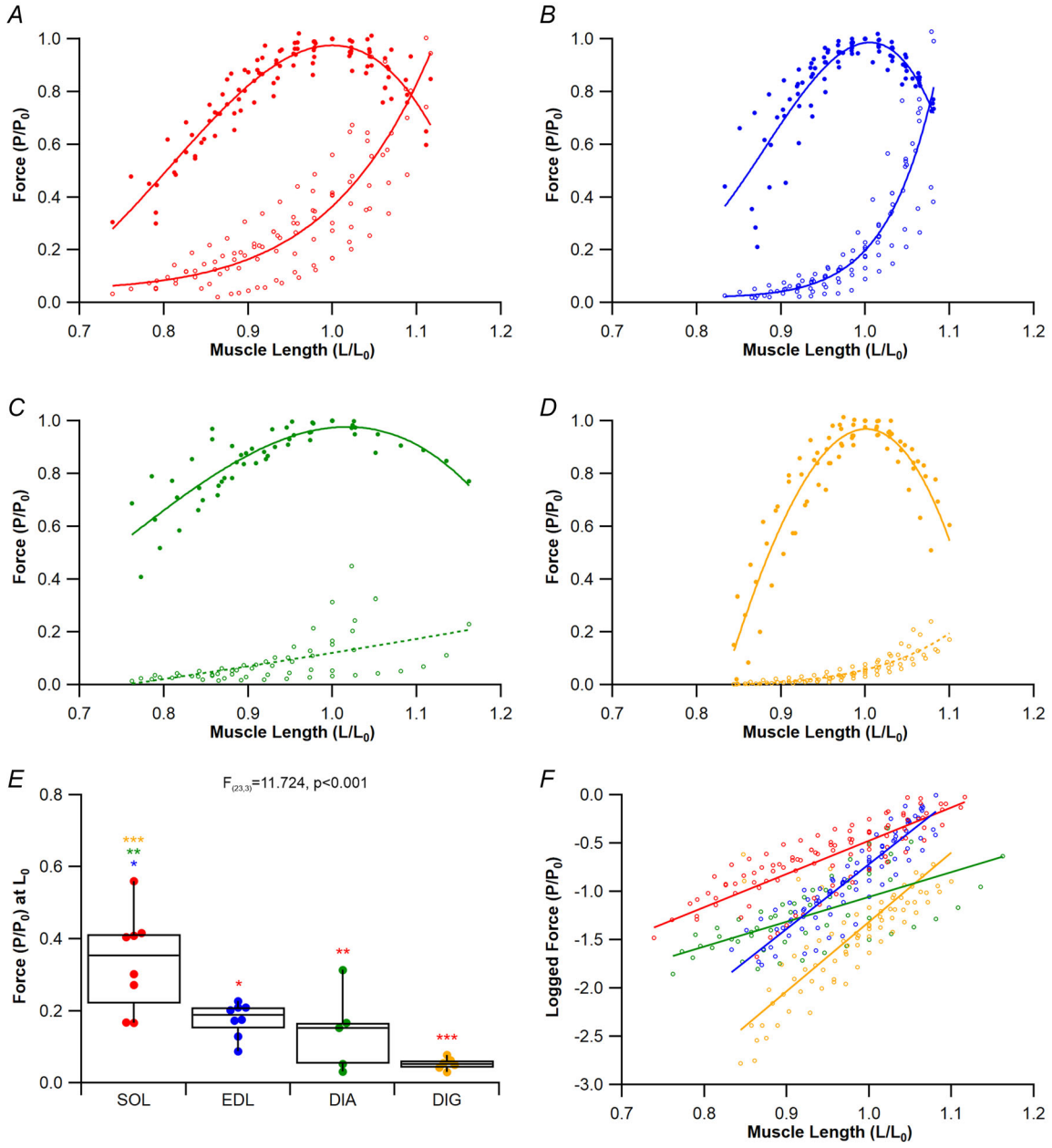

Figure 7. Active and passive muscle force–length relationship in different mammalian muscles
Force–length relationship for the soleus (*A*), extensor digitorum longus (*B*), diaphragm (*C*) and digastric (*D*) muscles for active (solid filled circles) and passive muscles (unfilled circles). Having analysed the eccentric force–velocity behaviour at L_0, we present the relative passive force at L_0 (*E*) highlighting the difference in passive muscle properties across the four muscles. Finally, the logged relative passive forces across the force–length relationship (*F*), further emphasising the differences in rate of passive force development. $^*P < 0.05$, $^{**}P < 0.01$, $^{***}P < 0.001$.

The inherent difficulty in characterising the eccentric force–velocity relationship

In previous investigations, there has been a lack of consistency in the experimental protocol used to investigate the eccentric force–velocity relationship. This has made it difficult to identify and characterise the eccentric muscle properties, which is required to develop reliable musculoskeletal models of muscle dynamic behaviours (Rajagopal et al., 2016). Many previous studies have completed eccentric ramps on the ascending limb of the force–length relationship (Krylow & Sandercock, 1997), whereas others have been conducted at non-physiological temperatures (Alcazar et al., 2019; Edman, 1988; Lännergren, 1978; Lombardi & Piazzesi, 1990), factors that are all considered to influence the eccentric force–velocity response (Alcazar et al., 2019). The lack of comprehensive data and standardised methodological approach has meant that approaches for modelling the eccentric force–velocity relationship in computational Hill-type musculoskeletal models have depended on narrow and arguably inappropriate sets of experimental data. For example, Millard et al. (2013) modelled the eccentric force–velocity relationship using data from an *in situ* preparation of the cat soleus muscle (Joyce et al., 1969) (at 37°C) and the *ex vivo* force–velocity relationship from the semi-tendinosus muscle of the frog (at 10°C) (Mashima et al., 1972).

Additionally, there has been no standardisation of the relative length on the force–length relationship that has been used to derive force for normalising the eccentric force–velocity relationship. This is problematic, given the biphasic force development response to stretch, because it is possible to produce dramatically different eccentric force–velocity relationships when taking just a single point value to define this relationship. While measuring the differential of relative force across phase-1 or phase-2 would yield a similar value regardless of measurement site as the two responses are virtually linear, and thus, less prone to error. We have demonstrated this to be a more reliable descriptor of the dynamic eccentric force–velocity relationship.

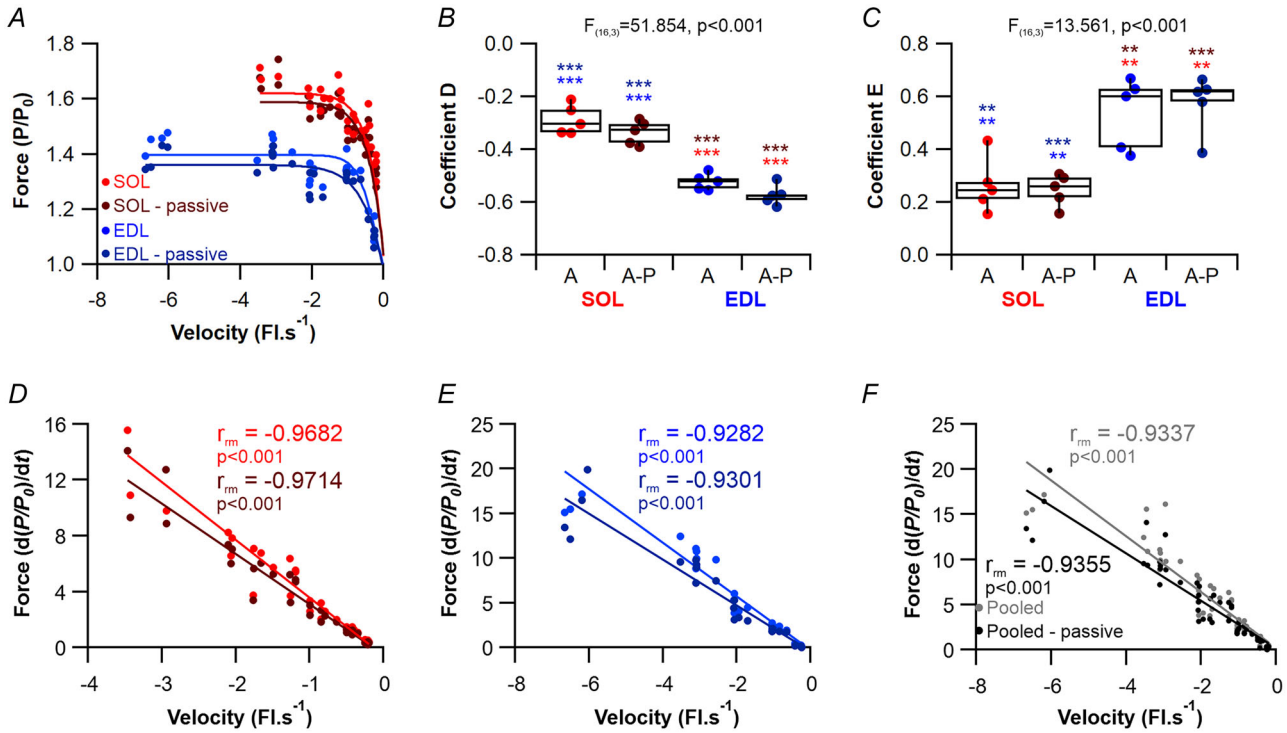

Figure 8. Effect of passive muscle properties during muscle lengthening of the mouse soleus and extensor digitorum longus muscles
A, eccentric force–velocity relationship for the SOL and EDL for the active data, and the active data minus passive eccentric ramps. *B*, there is a significant difference between the SOL and EDL coefficient *D*, but not between active *vs*. active minus passive force–velocity profiles. *C*, similarly, there is a significant difference between coefficient *E* of the SOL and the EDL, but no difference when accounting for passive force contribution during eccentric ramps. The relationship between $dx/dt/P_0$ remains significantly correlated with velocity for the SOL (*D*) and EDL (*E*); however, there is no effect when amending for passive force during the eccentric ramp. Finally, the pooled relationship between $dx/dt/P_0$ and lengthening velocity remains significantly correlated with velocity (*F*). $^*P < 0.05$, $^{**}P < 0.01$, $^{***}P < 0.001$.

Mechanistic underpinning of the eccentric biphasic force development response

It has long been established that shortening force–velocity properties differ between muscles that are predominantly fast- or slow contracting (Askew & Marsh, 1997), yet conflicting data exist on the eccentric force–velocity properties between fast- and slow-muscles, with some studies reporting no difference (Rijkelijkhuizen et al., 2003) and others reporting subtle velocity-specific differences (Ramsey et al., 2010; Stienen et al., 1992). Our data show that mouse SOL and EDL have significantly distinct muscle properties in terms of both the concentric and eccentric force–velocity relationships, with the SOL attaining a greater plateau height and more curved force–velocity profile compared to EDL during the eccentric force–velocity relationship. This observation appear to be consistent with those of Linari et al. (2004) who showed slow twitch fibres from humans to have a greater plateau height compared to fast twitch fibres. However, when comparing the rate of relative force development, both muscles appear to have similar profiles across normalised velocities. This is in contrast to the findings for muscles that were eccentrically stretched during cyclical contractions (Hessel & Nishikawa, 2017); however, the rate of change of force reported in the present study has been normalised to peak isometric force, whereas, in the study by Hessel and Nishikawa (2017), absolute forces were compared. Our findings here are further complicated when we consider the DIA and DIG that have a mixed fibre type composition. Both the DIA and DIG have a greater plateau height compared to that of the slow SOL, which suggests that this parameter is not underpinned by fibre phenotype. It is possible that the different relative stretch amplitude across our mammalian muscles may be masking subtle differences in muscle fibre phenotype (Josephson & Stokes, 1999; Krylow & Sandercock, 1997) and, as such, requires further exploration.

The physiological underpinning of the distinct biphasic force development response during eccentric lengthening is still a contentious topic. It is assumed that the initial rapid phase-1 profile is a response to elevated strain of attached cross-bridges, after which the detachment of myosin heads leads to the transition into a shallower phase-2 force response (Tomalka, 2023; Tomalka et al., 2020, 2021; Weidner et al., 2022), whereas the phase-2 force response is assumed to be linked to increased strain of non-cross-bridge parallel elastic elements (Ramsey et al., 2010; Tomalka, 2023). To the best of our knowledge, this is the first comprehensive overview of eccentric muscle characteristics in mammalian muscle. We have shown for the first time that the initial phase-1 response (i.e. cross-bridge activation) is velocity-dependent, and

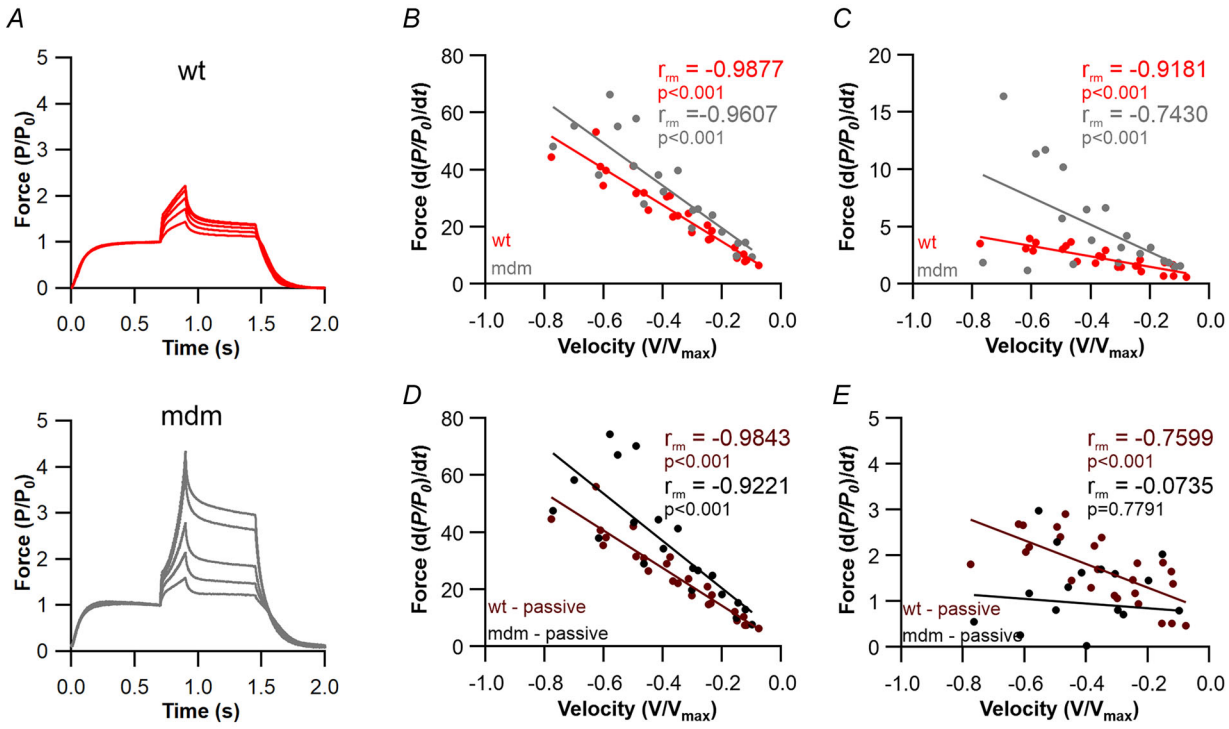

Figure 9. Contribution of titin to the eccentric force–velocity relationship in mouse soleus muscle
A, eccentric ramps during tetanic contractions for wild-type (wt) and titin knockout (mdm) soleus muscle. The rate of force development is shown as a function of normalised lengthening velocity across phase-1 (*B* and *D*) and phase-2 (*C* and *E*) on absolute force (*B* and *C*) and when accounting for passive force (*D* and *E*).

this relationship is conserved over three orders of magnitude of mammalian skeletal muscle mass. This may be indicative of a comparable proportion of cross-bridges are attached during the steep force rising phase-1. Additionally, we show that this rapid force development phase-1 response is neither affected by passive muscle properties, nor activation of titin, providing further support to the hypothesis that this is predominantly driven by cross-bridge activation. Interestingly, previous work on the dependence of the transition point between phase-1 and phase-2 has been inconclusive in establishing a relationship, with frog/toad muscles presenting with a biphasic velocity-dependent response that plateaus at ∼1.5 P/P_0, whereas the mouse soleus presented with a curvilinear velocity dependence (Stienen et al., 1992). We show here that, across our four mammalian muscles, there are significant linear relationships between the transition point and lengthening velocity.

Phase-2 of the force development profile has been equally under-investigated, despite it being routinely described in the literature (Josephson & Stokes, 1999; Joyce et al., 1969; Lombardi & Piazzesi, 1990; Stienen et al., 1992; Tomalka, 2023). Again, this is probably partly a result of the lack of standardised experimental approaches for muscle lengthening experimentation and quantification. Our data show that there is a significant relationship with the rate of force development and velocity of muscle lengthening for phase-2 of the force development response. This response does not appear to be affected by passive muscle properties, but is reliant on normal titin activation. The SOL and EDL express different titin isoforms (Hettige et al., 2022), which have been proposed to affect passive forces differentially (Prado et al., 2005), yet they presented with comparable rates of force development across phase-2 of the eccentric ramp. There are several possible reasons for this. First, it may be that different titin isoforms do not play a role in the rate of force development during stretch but are integral to the level of force enhancement following cessation of stretch. Alternatively, this may suggest that additional, non-contractile elements contribute to this force enhancement (Hettige et al., 2020, 2022; Prado et al., 2005).

Our data provide a novel insight into the dynamic force enhancement response to muscle stretch. In the first case, our collective mammalian data suggest that the current default Hill-type musculoskeletal model of the eccentric force–velocity relationship, which plateaus at 1.40 P/P_0 (Millard et al., 2013), is actually underestimating the plateau by 18% (our average mammalian plateau occurs at 1.65 P/P_0). Additionally, the current representation of the eccentric force–velocity as a hyperbolic fit may be too simplistic given the dynamic biphasic response of muscle force to stretch and therefore musculoskeletal models should incorporate the rate of force development. The data presented here enable the calculation of the transition between the rapid force development of phase-1 and the shallower phase-2. These data may provide a foundational step towards improving Hill type musculoskeletal model predictions; however, this relationship has only been validated in maximally activated muscles, and this relationship may not represent the true eccentric biphasic response under normal physiological recruitment.

Experimental limitations

The lack of consistency in the experimental protocols that have been used to study the eccentric force–velocity relationship makes it inherently difficult to critically compare data between studies. For example, many previous studies have conducted eccentric ramps at different positions (relative to L_0) on the force–length relationship with some studies performing contractions entirely on the ascending limb and never crossing L_0 (Krylow & Sandercock, 1997), while others have used lengthening contractions that occur symmetrically across L_0 (Tahir et al., 2020) but have varied strain. While we have consistently subjected our four mammalian muscles to symmetrical length excursions across L_0 for each of these muscles, the relative strain each muscle was subjected to was not equal, and as such the variability presented here may be in part a consequence of this. Rat muscles stretched at the same velocity at different positions on the ascending limb of the force–length relationship show a shift in the transition point between the phase-1 and phase-2 force profiles (Krylow & Sandercock, 1997) as well as the plateau of the eccentric side of the force–velocity relationship. However, it should be noted that these data were presented as absolute force, in contrast to the data we report, which has been normalised to P_0, the impact of which is currently unknown. There is an inherent difficulty in generating a standardised approach to assess the eccentric force–velocity relationship in whole muscle preparations. Simply using a constant strain across L_0 (e.g. ±10% L_0) could be argued inappropriate. Our data (Fig. 8) highlight the significant difference in the force–length relationships across mammalian muscle (Mendoza et al., 2023), with for example a ± 10% L_0 strain on the DIG muscle would descend down the ascending/descending limb to as low as 60% of P_0 while the same strain in the DIA would not drop below 80% of P_0. More work is required to comprehensively characterise the importance of position on the force–length relationship on the eccentric behaviour of muscle (Krylow & Sandercock, 1997; Tomalka et al., 2017). Further, complications arise when considering the method with which eccentric muscle properties are derived, as previously noted differences may exist in the force–velocity profiles when derived from isovelocity or from isotonic experimentation

(Woledge et al., 1985). While our data here are derived from isovelocity experiments like those used to develop default OpenSim parameters (Millard et al., 2013) the sensitivity of these models to data derived from isovelocity and isotonic approaches are unknown. This poses compelling consideration for incorporation of these data into Hill type musculoskeletal models, and highlights many avenues for future work.

In conclusion, our standardised approach has shown there to be a conserved relationship between the velocity of muscle lengthening and the rate of force development across mammalian muscle. The characterisation of the rate of force development of the biphasic force response may be a more reliable way to describe the forces during eccentric muscle contractions compared to the traditional hyperbolic curve fitting. Our data support the hypothesis that the rapid force (phase-1) development during muscle lengthening is a function of cross-bridge activation while the slower phase of force development (phase-2) is reliant on titin activation.

Appendix

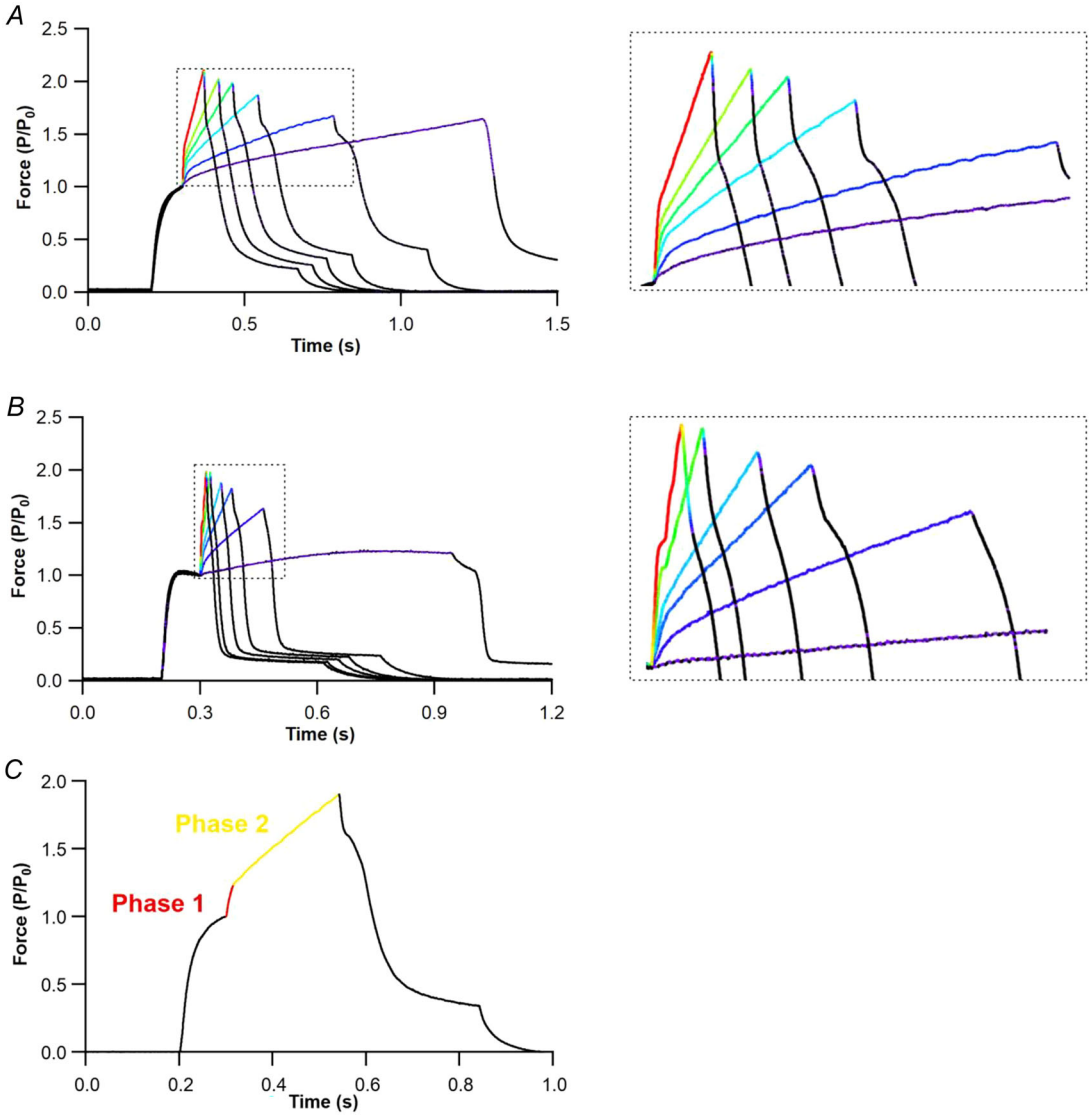

Figure A1. Example eccentric plots
Isovelocity lengthening from a single animal, for the soleus (*A*) and extensor digitorum longus (*B*). Expanded regions emphasise the two-phase response of both muscles during lengthening. These comprise of a phase of rapid force development (phase-1) and a phase of slow force development (phase-2) (*C*).

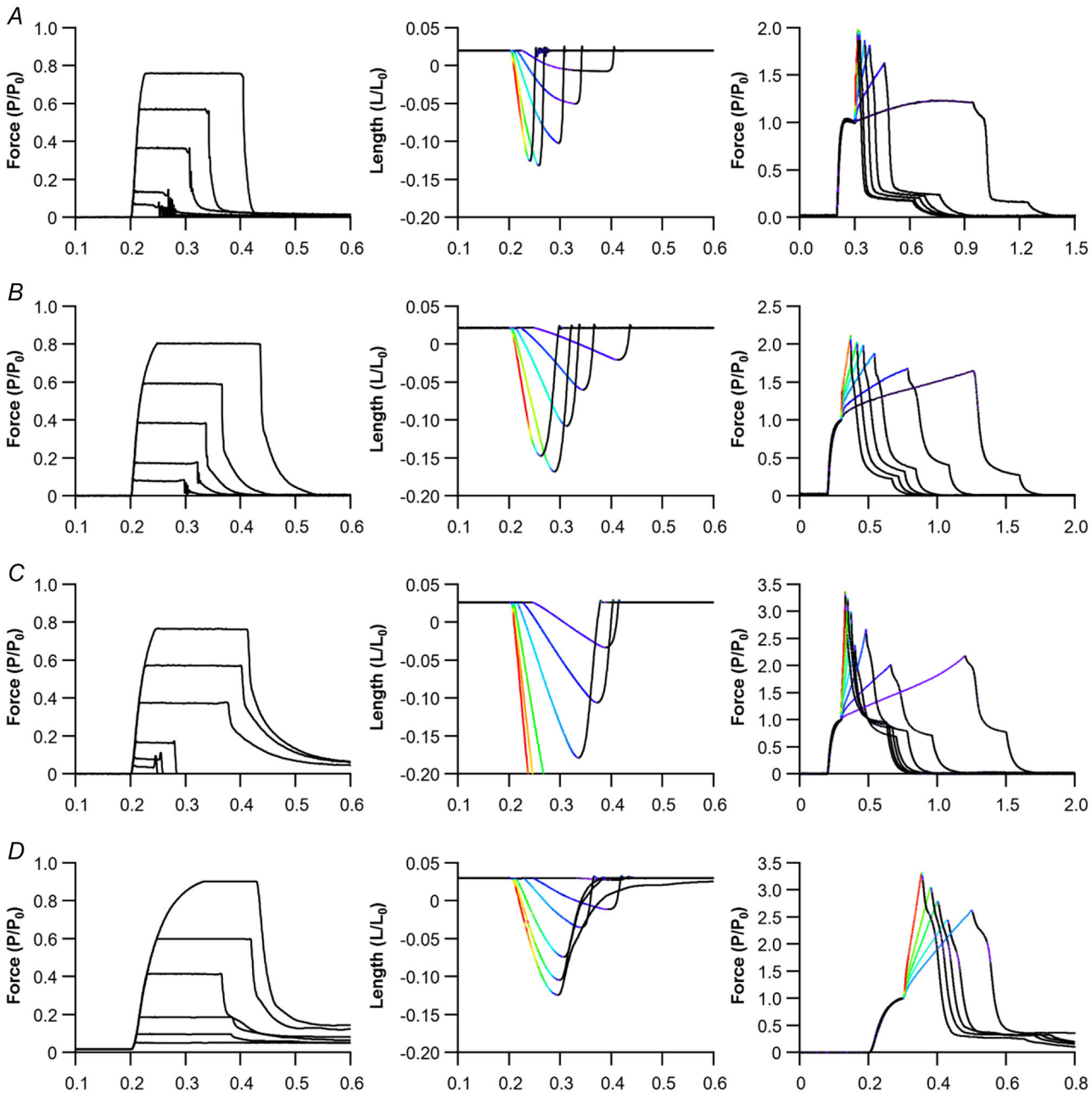

Figure A2. Example concentric and eccentric force plots
Example force (left) and length (middle) profiles during isotonic shortening (concentric) experiments for the mouse soleus (*A*), mouse extensor digitorum longus (*B*), rat diaphragm (*C*) and rabbit digastric muscle (*D*). Example iso-velocity lengthening (eccentric) force profiles for these muscles are presented in the right-hand column. Heat map colours correspond the velocity of either muscle shortening or lengthening.

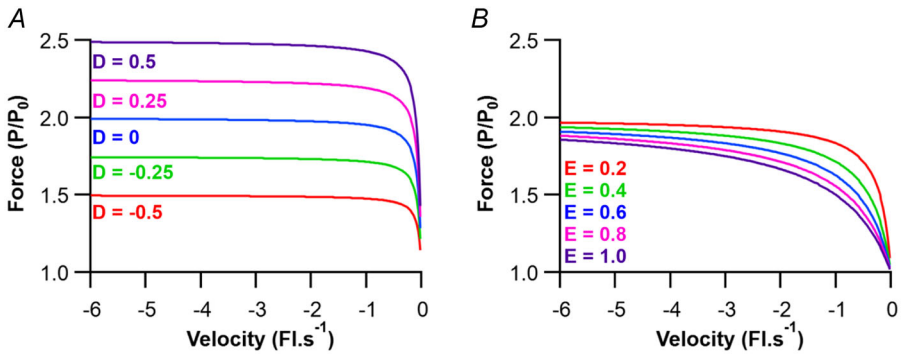

Figure A3. Coefficients of the eccentric force–velocity equation
Changes in coefficient *D* alter the plateau height of the eccentric force–velocity fit (*A*), whereas changes in the *E* coefficient vary the curvature of this relationship (*B*). Coefficient *E* was fixed at 0.05 in (*A*), whereas coefficient *D* was fixed at 0 in (*B*).

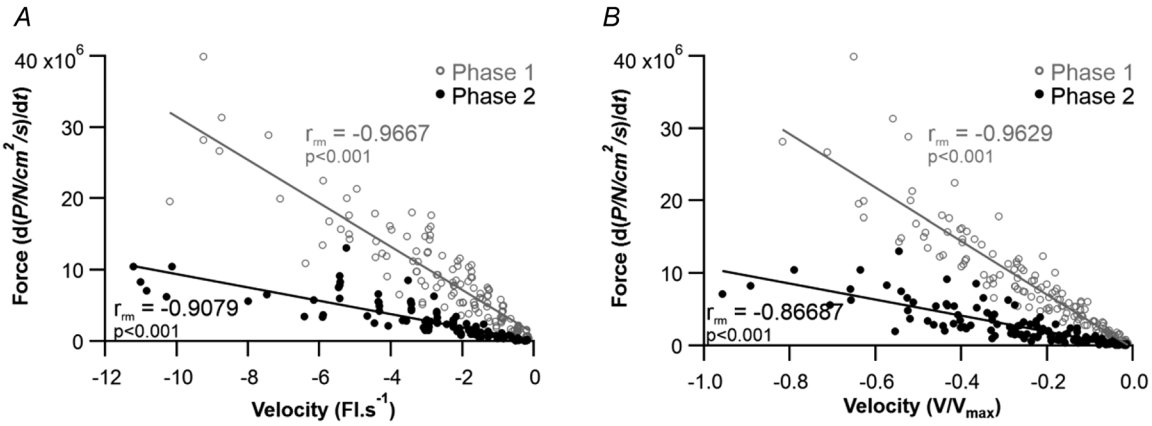

Figure A4. Pooled rate of force development relative to physiological cross-sectional area
Pooled rate of force development as a function of absolute lengthening velocity (*A*) and normalised lengthening velocity (*B*) across phase one (grey) and phase two (black) (*B*) of the isovelocity lengthening relationship. $*P < 0.05$, $**P < 0.01$, $***P < 0.001$.

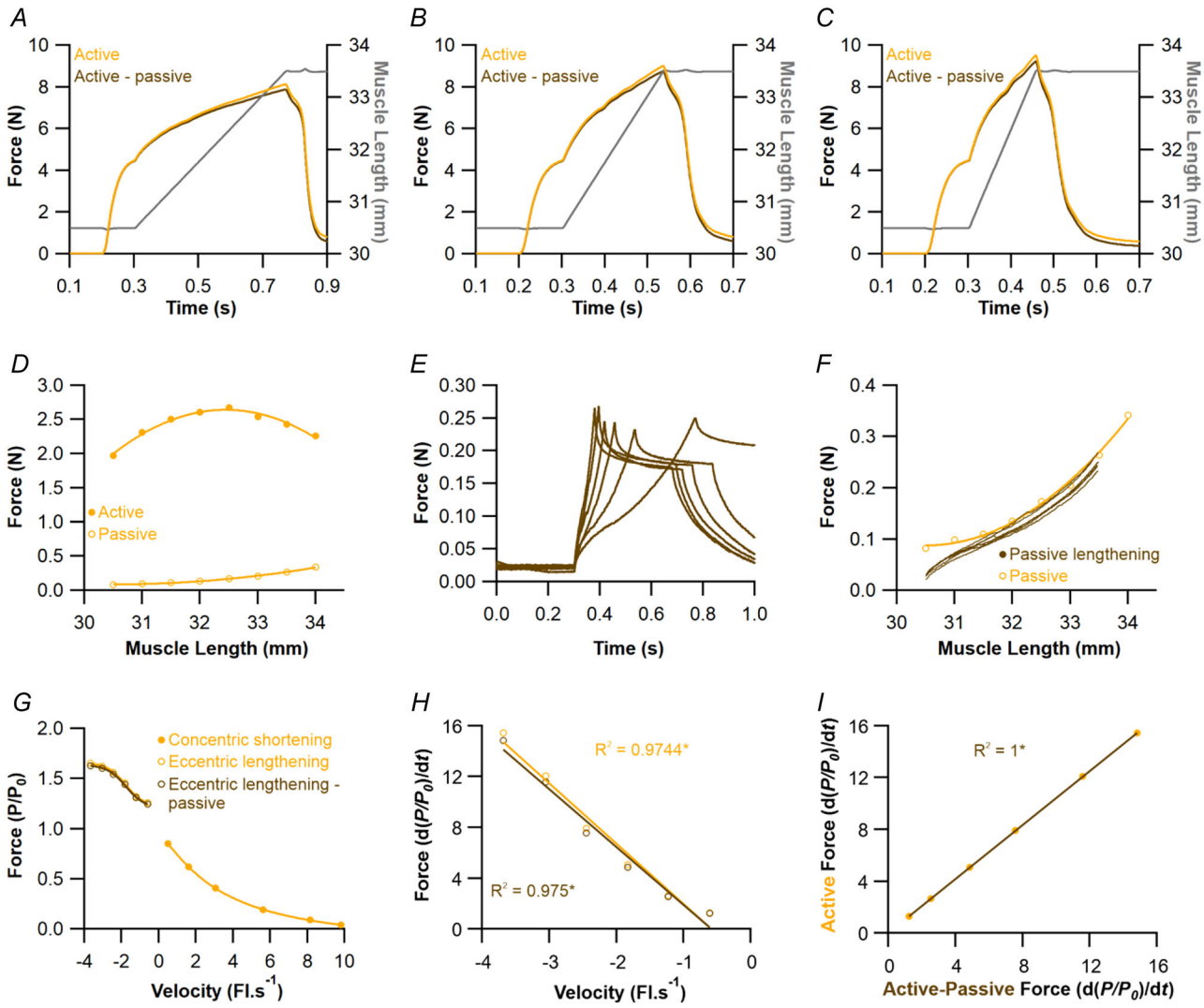

Figure A5. Passive muscle properties during muscle lengthening of the rabbit digastric muscle
Example muscle forces during lengthening at −0.61 (*A*), −1.22 (*B*) and −1.83 Fl s^{-1} (*C*) for absolute forces (orange) and active forces minus passive forces (brown) from a single digastric muscle. Muscle specific isometric twitch force–length relationship (*D*). Muscle forces during six passive lengthening ramps at different velocities (brown) (*E*). Passive force length data (taken from *D*) are plot again passive ramp forces (taken from *E*), which overlap with the isometric passive force (orange) (*F*). These data highlight the independence of passive force properties to the velocity of stretch. Eccentric (unfilled circles) and concentric (filled circles) force–velocity relationship, with active (orange) and active minus passive (brown) eccentric plots showing a similar relationship (*G*). The correlation for the phase-2 d(P/P_0)/dt *vs.* velocity shows a comparable rate of force development for both the active (orange) and the active minus the passive forces (brown) (*H*) and when correlated together show a linear relationship (*I*).

References

Alcazar, J., Csapo, R., Ara, I., & Alegre, L. M. (2019). On the shape of the force-velocity relationship in skeletal muscles: The linear, the hyperbolic, and the double-hyperbolic. *Frontiers in Physiology*, **10**, 769.

Altringham, J. D., & Young, I. S. (1991). Power output and the frequency of oscillatory work in mammalian diaphragm muscle: The effects of animal size. *Journal of Experimental Biology*, **157**(1), 381–389.

Askew, G. N. (2023). Adaptations for extremely high muscular power output: Why do muscles that operate at intermediate cycle frequencies generate the highest powers? *Journal of Muscle Research and Cell Motility*, **44**(2), 107–114.

Askew, G. N., & Marsh, R. L. (1997). The effects of length trajectory on the mechanical power output of mouse skeletal muscles. *Journal of Experimental Biology*, **200**(24), 3119–3131.

Askew, G. N., & Marsh, R. L. (2001). The mechanical power output of the pectoralis muscle of blue-breasted quail (Coturnix chinensis): The in vivo length cycle and its implications for muscle performance. *Journal of Experimental Biology*, **204**(21), 3587–3600.

Askew, G. N., Young, I. S., & Altringham, J. D. (1997). Fatigue of mouse soleus muscle, using the work loop technique. *Journal of Experimental Biology*, **200**(22), 2907–2912.

Azizi, E. (2014). Locomotor function shapes the passive mechanical properties and operating lengths of muscle. *Proceedings of the Royal Society B: Biological Sciences*, **281**, 20132914.

Bakdash, J. Z., & Marusich, L. R. (2017). Repeated measures correlation. *Frontiers in Psychology*, **8**, 00456.

Barclay, C. J. (1996). Mechanical efficiency and fatigue of fast and slow muscles of the mouse. *The Journal of Physiology*, **497**(3), 781–794.

Blum, K. P., Campbell, K. S., Horslen, B. C., Nardelli, P., Housley, S. N., Cope, T. C., & Ting, L. H. (2020). Diverse and complex muscle spindle afferent firing properties emerge from multiscale muscle mechanics. *Elife*, **9**, e55177.

Blum, K. P., Lamotte D'incamps, B., Zytnicki, D., & Ting, L. H. (2017). Force encoding in muscle spindles during stretch of passive muscle. *PLoS Computational Biology*, **13**(9), e1005767.

Burton, R. F. (1975). *Ringer solutions and physiological salines*. Wright-Scientechnica.

Charles, J., Kissane, R., Hoehfurtner, T., & Bates, K. T. (2022). From fibre to function: Are we accurately representing muscle architecture and performance? *Biological Reviews*, **97**(4), 1640–1676.

Dantuma, R., & Weijs, W. A. (1980). Functional anatomy of the masticatory apparatus in the rabbit (Oryctolagus cuniculus L.). *Netherlands Journal of Zoology*, **31**(1), 99–147.

De Ruiter, C. J., Didden, W. J. M., Jones, D. A., & De Haan, A. (2000). The force-velocity relationship of human adductor pollicis muscle during stretch and the effects of fatigue. *The Journal of physiology*, **526**(3), 671.

Edman, K. A. (1988). Double-hyperbolic force-velocity relation in frog muscle fibres. *The Journal of Physiology*, **404**(1), 301–321.

Edman, K. A., Elzinga, G., & Noble, M. I. (1978). Enhancement of mechanical performance by stretch during tetanic contractions of vertebrate skeletal muscle fibres. *The Journal of Physiology*, **281**(1), 139–155.

Espino-Gonzalez, E., Tickle, P. G., Benson, A. P., Kissane, R. W. P., Askew, G. N., Egginton, S., & Bowen, T. S. (2021). Abnormal skeletal muscle blood flow, contractile mechanics and fibre morphology in a rat model of obese-HFpEF. *The Journal of Physiology*, **599**(3), 981–1001.

Gillis, G. B., & Biewener, A. A. (2001). Hindlimb muscle function in relation to speed and gait: In vivo patterns of strain and activation in a hip and knee extensor of the rat (Rattus norvegicus). *Journal of Experimental Biology*, **204**(15), 2717–2731.

Gillis, G. B., Flynn, J. P., Mcguigan, P., & Biewener, A. A. (2005). Patterns of strain and activation in the thigh muscles of goats across gaits during level locomotion. *Journal of Experimental Biology*, **208**(24), 4599–4611.

Grundy, D. (2015). *Principles and standards for reporting animal experiments in The Journal of Physiology and Experimental Physiology* (pp. 755–758). Wiley Online Library.

Herzog, W. (2014). The role of titin in eccentric muscle contraction. *Journal of Experimental Biology*, **217**(16), 2825–2833.

Herzog, W., Schappacher, G., Duvall, M., Leonard, T. R., & Herzog, J. A. (2016). Residual force enhancement following eccentric contractions: A new mechanism involving titin. *Physiology*, **31**(4), 300–312.

Hessel, A. L., & Nishikawa, K. C. (2017). Effects of a titin mutation on negative work during stretch–shortening cycles in skeletal muscles. *Journal of Experimental Biology*, **220**, 4177–4185.

Hettige, P., Mishra, D., Granzier, H., Nishikawa, K., & Gage, M. J. (2022). Contributions of titin and collagen to passive stress in muscles from mdm mice with a small deletion in titin's molecular spring. *International Journal of Molecular Sciences*, **23**(16), 8858.

Hettige, P., Tahir, U., Nishikawa, K. C., & Gage, M. J. (2020). Comparative analysis of the transcriptomes of EDL, psoas, and soleus muscles from mice. *Biomedical Central Genomics [Electronic Resource]*, **21**(1), 1–16.

Hill, A. V. (1938). The heat of shortening and the dynamic constants of muscle. *Proceedings of the Royal Society of London Series B-Biological Sciences*, **126**, 136–195.

Holt, N. C., & Askew, G. N. (2012). The effects of asymmetric length trajectories on the initial mechanical efficiency of mouse soleus muscles. *The Journal of Experimental Biology*, **215**(2), 324–330.

Josephson, R. K., & Stokes, D. R. (1999). The force-velocity properties of a crustacean muscle during lengthening. *Journal of Experimental Biology*, **202**(5), 593–607.

Joyce, G. C., Rack, P. M. H., & Westbury, D. R. (1969). The mechanical properties of cat soleus muscle during controlled lengthening and shortening movements. *The Journal of Physiology*, **204**(2), 461–474.

Katz, B. (1939). The relation between force and speed in muscular contraction. *The Journal of Physiology*, **96**(1), 45.

Kissane, R. W. P., Charles, J. P., Banks, R. W., & Bates, K. T. (2022). Skeletal muscle function underpins muscle spindle abundance. *Proceedings of the Royal Society B*, **289**(1976), 20220622.

Kissane, R. W. P., Charles, J. P., Banks, R. W., & Bates, K. T. (2023). The association between muscle architecture and muscle spindle abundance. *Scientific Reports*, **13**(1), 2830.

Kissane, R. W. P., Egginton, S., & Askew, G. N. (2018). Regional variation in the mechanical properties and fibre-type composition of the rat extensor digitorum longus muscle. *Experimental Physiology*, **103**(1), 111–124.

Kissane, R. W. P., Wright, O., Al'Joboori, Y. D., Marczak, P., Ichiyama, R. M., & Egginton, S. (2019). Effects of treadmill training on microvascular remodeling in the rat after spinal cord injury. *Muscle & Nerve*, **59**, 370–379.

Krylow, A. M., & Sandercock, T. G. (1997). Dynamic force responses of muscle involving eccentric contraction. *Journal of Biomechanics*, **30**(1), 27–33.

Lai, A. K. M., Biewener, A. A., & Wakeling, J. M. (2019). Muscle-specific indices to characterise the functional behaviour of human lower-limb muscles during locomotion. *Journal of Biomechanics*, **89**, 134–138.

Lännergren, J. (1978). The force—velocity relation of isolated twitch and slow muscle fibres of Xenopus laevis. *The Journal of Physiology*, **283**(1), 501–521.

Linari, M., Bottinelli, R., Pellegrino, M. A., Reconditi, M., Reggiani, C., & Lombardi, V. (2004). The mechanism of the force response to stretch in human skinned muscle fibres with different myosin isoforms. *The Journal of Physiology*, **554**(2), 335–352.

Lombardi, V., & Piazzesi, G. (1990). The contractile response during steady lengthening of stimulated frog muscle fibres. *The Journal of Physiology*, **431**(1), 141–171.

Luff, A. R. (1981). Dynamic properties of the inferior rectus, extensor digitorum longus, diaphragm and soleus muscles of the mouse. *The Journal of Physiology*, **313**(1), 161.

Marsh, R. L., & Bennett, A. F. (1986). Thermal dependence of contractile properties of skeletal muscle from the lizard Sceloporus occidentalis with comments on methods for fitting and comparing force-velocity curves. *Journal of Experimental Biology*, **126**(1), 63–77.

Mashima, H., Akazawa, K., Kushima, H., & Fujii, K. (1972). The force-load-velocity relation and the viscous-like force in the frog skeletal muscle. *The Japanese Journal of Physiology*, **22**(1), 103–120.

Mayerl, C. J., Steer, K. E., Chava, A. M., Bond, L. E., Edmonds, C. E., Gould, F. D. H., Stricklen, B. M., Hieronymous, T. L., & German, R. Z. (2021). The contractile patterns, anatomy and physiology of the hyoid musculature change longitudinally through infancy. *Proceedings of the Royal Society B*, **288**(1946), 20210052.

McFarlane, L., Altringham, J. D., & Askew, G. N. (2016). Intra-specific variation in wing morphology and its impact on take-off performance in blue tits (Cyanistes caeruleus) during escape flights. *Journal of Experimental Biology*, **219**, 1369–1377.

Mendoza, E., Moen, D. S., & Holt, N. C. (2023). The importance of comparative physiology: Mechanisms, diversity and adaptation in skeletal muscle physiology and mechanics. *Journal of Experimental Biology*, **226**(1), jeb245158.

Millard, M., Uchida, T., Seth, A., & Delp, S. L. (2013). Flexing computational muscle: Modeling and simulation of musculotendon dynamics. *Journal of Biomechanical Engineering*, **135**(2),

Pellegrino, M. A., Canepari, M., Rossi, R., D'antona, G., Reggiani, C., & Bottinelli, R. (2003). Orthologous myosin isoforms and scaling of shortening velocity with body size in mouse, rat, rabbit and human muscles. *The Journal of Physiology*, **546**(3), 677–689.

Percie du Sert, N., Hurst, V., Ahluwalia, A., Alam, S., Avey, M. T., Baker, M., Browne, W. J., Clark, A., Cuthill, I. C., & Dirnagl, U. (2020). The ARRIVE guidelines 2.0: Updated guidelines for reporting animal research. *Journal of Cerebral Blood Flow & Metabolism*, **40**, 1769–1777.

Pinniger, G. J., Ranatunga, K. W., & Offer, G. W. (2006). Crossbridge and non-crossbridge contributions to tension in lengthening rat muscle: Force-induced reversal of the power stroke. *The Journal of Physiology*, **573**(3), 627–643.

Powers, K., Nishikawa, K., Joumaa, V., & Herzog, W. (2016). Decreased force enhancement in skeletal muscle sarcomeres with a deletion in titin. *Journal of Experimental Biology*, **219**, 1311–1316.

Prado, L. G., Makarenko, I., Andresen, C., KrüGer, M., Opitz, C. A., & Linke, W. A. (2005). Isoform diversity of giant proteins in relation to passive and active contractile properties of rabbit skeletal muscles. *The Journal of General Physiology*, **126**(5), 461–480.

Rajagopal, A., Dembia, C. L., Demers, M. S., Delp, D. D., Hicks, J. L., & Delp, S. L. (2016). Full-body musculoskeletal model for muscle-driven simulation of human gait. *Institute of Electrical and Electronics Engineers Transactions on Biomedical Engineering*, **63**(10), 2068–2079.

Ramsey, K. A., Bakker, A. J., & Pinniger, G. J. (2010). Fiber-type dependence of stretch-induced force enhancement in rat skeletal muscle. *Muscle & Nerve*, **42**, 769–777.

Rijkelijkhuizen, J. M., De Ruiter, C. J., Huijing, P. A., & De Haan, A. (2003). Force/velocity curves of fast oxidative and fast glycolytic parts of rat medial gastrocnemius muscle vary for concentric but not eccentric activity. *Pflügers Archiv*, **446**(4), 497–503.

Roberts, T. J., Higginson, B. K., Nelson, F. E., & Gabaldón, A. M. (2007). Muscle strain is modulated more with running slope than speed in wild turkey knee and hip extensors. *Journal of Experimental Biology*, **210**(14), 2510–2517.

Stienen, G. J., Versteeg, P. G., Papp, Z., & Elzinga, G. (1992). Mechanical properties of skinned rabbit psoas and soleus muscle fibres during lengthening: Effects of phosphate and Ca^{2+}. *The Journal of Physiology*, **451**(1), 503–523.

Tahir, U., Monroy, J. A., Rice, N. A., & Nishikawa, K. C. (2020). Effects of a titin mutation on force enhancement and force depression in mouse soleus muscles. *Journal of Experimental Biology*, **223**(2), jeb197038.

Tomalka, A. (2023). Eccentric muscle contractions: From single muscle fibre to whole muscle mechanics. *Pflügers Archiv-European Journal of Physiology*, **475**(4), 421–435.

Tomalka, A., Rode, C., Schumacher, J., & Siebert, T. (2017). The active force–length relationship is invisible during extensive eccentric contractions in skinned skeletal muscle fibres. *Proceedings of the Royal Society B: Biological Sciences*, **284**(1854), 20162497.

Tomalka, A., Weidner, S., Hahn, D., Seiberl, W., & Siebert, T. (2020). Cross-bridges and sarcomeric non-cross-bridge structures contribute to increased work in stretch-shortening cycles. *Frontiers in Physiology*, **11**, 921.

Tomalka, A., Weidner, S., Hahn, D., Seiberl, W., & Siebert, T. (2021). Power amplification increases with contraction velocity during stretch-shortening cycles of skinned muscle fibers. *Frontiers in Physiology*, **12**, 644981.

Usherwood, J. R. (2022). Legs as linkages: An alternative paradigm for the role of tendons and isometric muscles in facilitating economical gait. *Journal of Experimental Biology*, **225**(1), jeb243254.

Warren, P. M., Kissane, R. W. P., Egginton, S., Kwok, J. C. F., & Askew, G. N. (2021). Oxygen transport kinetics underpin rapid and robust diaphragm recovery following chronic spinal cord injury. *The Journal of Physiology*, **599**, 1199–1224.

Weidner, S., Tomalka, A., Rode, C., & Siebert, T. (2022). How velocity impacts eccentric force generation of fully activated skinned skeletal muscle fibers in long stretches. *Journal of Applied Physiology*, **133**(1), 223–233.

Woledge, R. C., Curtin, N. A., & Homsher, E. (1985). Energetic aspects of muscle contraction. *Monographs of the Physiological Society*, **41**, 1–357.

Additional information

Data availability statement

Data are available via the University of Liverpool's Data Repository (https://datacat.liverpool.ac.uk/id/eprint/2427).

Competing interests

The authors declare that they have no competing interests.

Author contributions

R.W.P.K. and G.N.A. were responsible for conceptualisation. R.W.P.K. and G.N.A. were responsible for methodology. R.W.P.K. was responsible for formal analysis. R.W.P.K. was responsible for writing the original draft. G.N.A. was responsible for reviewing and editing. R.W.P.K. and G.N.A. were responsible for funding acquisition.

Funding

This research was supported by a BBSRC Project Grant (BB/R016917/1) to G.N.A. This work was also supported by an internal funding scheme funded by the Wellcome Trust Institutional Strategic Support Fund grant (204 822/Z/16/Z) and awarded to RWPK by the Faculty of Health and Life Sciences, University of Liverpool.

Keywords

force–velocity, lengthening, muscle mechanics, scaling, titin

Supporting information

Additional supporting information can be found online in the Supporting Information section at the end of the HTML view of the article. Supporting information files available:

Peer Review History